Biochimica et Biophysica Acta 1861 (2017) 218–234

Contents lists available at ScienceDirect

Biochimica et Biophysica Acta

journal homepage: www.elsevier.com/locate/bbagen

Synthesis, biological characterization and evaluation of molecular mechanisms of novel copper complexes as anticancer agents

Ceyda Acilan [a,*], Buse Cevatemre [b,1], Zelal Adiguzel [a,1], Didem Karakas [b], Engin Ulukaya [c], Nádia Ribeiro [d], Isabel Correia [d,*], João Costa Pessoa [d]

[a] TUBITAK, Marmara Research Center, Genetic Engineering and Biotechnology Institute, Gebze, Kocaeli, Turkey
[b] Uludag University, Faculty of Arts and Sciences, Department of Biology, Bursa, Turkey
[c] Uludag University, Medical School, Department of Medical Biochemistry, Bursa, Turkey
[d] Centro de Química Estrutural, Instituto Superior Técnico, Universidade de Lisboa, Av. Rovisco Pais 1, 1049-001 Lisbon, Portugal

ARTICLE INFO

Article history:
Received 6 June 2016
Received in revised form 30 September 2016
Accepted 18 October 2016
Available online 20 October 2016

Keywords:
Copper complexes
Schiff base compounds
Phenanthroline
Interactions with DNA
Anti-cancer drugs
Mechanism of cytotoxicity of Cu-compounds

ABSTRACT

Background: To overcome the hurdles of cisplatin, majorly its toxicity and resistance, there has been extensive search for alternative anti-cancer metal-based compounds. Here, three Cu(II)-complexes, Cu(Sal-Gly)(phen), Cu(Sal-Gly)(pheamine), Cu(Sal-Gly)(phepoxy) are characterized for their interaction with DNA, cytotoxicity and mechanism of action.
Methods: The binding ability of the complexes to Calf-Thymus DNA was evaluated by competition fluorescence studies with thiazole-orange, UV–Vis and circular dichroism spectroscopic titrations. Cytotoxicity was evaluated by MTT analysis. The DNA damage was analyzed through cleavage of supercoiled DNA via agarose gel-electrophoresis, and 8-oxo-guanidine and γH2AX staining in cells. Apoptosis was detected via DNA condensation/fragmentation, mitochondrial membrane potential, Annexin V staining and caspase 3/7 activity. Formation of reactive oxygen species was determined by DCFDA- and GSSG/GSH-analysis.
Results: Binding constants to DNA were evaluated as 1.7×10^6 (Cu(Sal-Gly)(phen)), 2.5×10^6 (Cu(Sal-Gly)(pheamine)) and 3.2×10^5 (Cu(Sal-Gly)(phepoxy)). All compounds induced DNA damage. Apoptosis was the main form of cell death. There was an increase in ROS, which is most likely responsible for the observed DNA-damage. Although the compounds were cytotoxic to all tested cancer cell lines, only Cu(Sal-Gly)(pheamine) displayed significantly lower toxicity towards non-cancer cells, its associated phenotypes differing from the other two Cu-complexes. Thus, Cu(Sal-Gly)(pheamine) was further assayed for molecular changes in response to drug treatment using a custom designed RT-qPCR array. Results showed that Harakiri was significantly upregulated. Presence of p53 was not required for apoptosis in response to Cu-complexes.
Conclusions and general significance: These Cu-complexes, namely Cu(Sal-Gly)(pheamine), may be considered promising anticancer agents with activity in cancer cells even with deficient p53 status.
© 2016 Published by Elsevier B.V.

1. Introduction

Metal-based molecules offer huge possibilities for the design of therapeutic agents not accessible to organic compounds; and cisplatin, which is prescribed to almost half of the cancer patients [1,2], is still regarded as one of the most important drugs in anticancer therapy. Despite its success, its clinical use is limited due to severe side effects, in addition to intrinsic or acquired resistance to cisplatin. These limitations triggered an exponential growth in the development of alternative metal-based drugs bearing metal ions other than platinum, which allow alternative mechanisms of action, and might have improved anticancer activity.

Among the non-platinum based compounds, copper complexes have received particular attention. Copper is an essential element for humans and most aerobic organisms [3,4]. It is important for the function of several enzymes and proteins involved in energy metabolism, respiration, and DNA synthesis [5], and most Cu-based complexes have been investigated on the assumption that endogenous metal ions may be less toxic for normal cells, than to cancer cells. Cu-complexes can easily undergo redox reactions [6], and furthermore, cancer cells have showed increased Cu uptake [7,8]. Based on these observations, Cu-compounds are expected to be less toxic, while retaining effective cytotoxicity towards cancer cells [9].

The majority of compounds developed so far are mononuclear Cu^{II}-species [9,10]; their mode of action is miscellaneous but differs

* Correspondence authors.
E-mail addresses: ceyda.acilan@tubitak.gov.tr (C. Acilan), icorreia@tecnico.ulisboa.pt (I. Correia).
[1] These authors contributed equally to this work.

http://dx.doi.org/10.1016/j.bbagen.2016.10.014
0304-4165/© 2016 Published by Elsevier B.V.

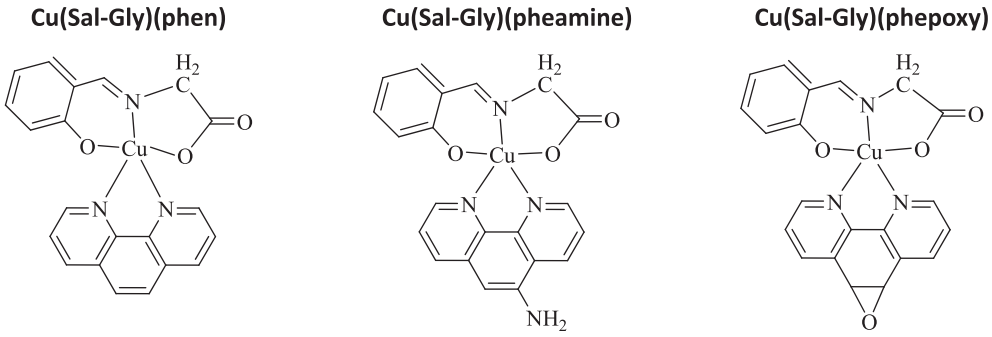

Fig. 1. Molecular structures of the three Cu-complexes studied.

from that of cisplatin; it includes DNA interaction, mitochondrial toxicity and ROS generation [3,9–11]. Depending on the Cu-complex size, charge, electron affinity and ability for adduct formation, Cu-compounds may also bind to biomembranes leading to cytotoxicity [12].

A great variety of Cu-complexes has been tested as cytotoxic agents and showed antitumor activity in several in vitro tests and a few in vivo experiments [3,5], namely 2,2′-bipyridine (bipy) and 1,10-phenanthroline (phen) containing complexes [13–19]. Regarding DNA interaction, the compounds containing phen have been reported to bind DNA by intercalative and non-intercalative interactions, either as free ligands or included in the metal complex [11]. Overall, they have been proposed as agents for binding, cleavage and oxidative modification of DNA [19–23].

In this study, we aimed to determine the cytotoxicity and molecular mechanism of action of three Cu^{II}-complexes. Cu(Sal-Gly)(phen) was synthesized by our group and showed promising cytotoxicity in breast cancer cells [19]. Here, we further characterize this complex and two novel derivatives, Cu(Sal-Gly)(pheamine) and Cu(Sal-Gly)(phepoxy) (Fig. 1), for their cytotoxicity in a broader spectrum of cancer cell lines, DNA binding properties and biological mechanism of action, aiming to be able to design agents with improved drug activity. DNA condensation/fragmentation, assessment of Annexin V staining, caspase 3/7 activity and mitochondrial membrane potential (MMP) were evaluated. Cu(Sal-Gly)(pheamine) was further tested for differential expression of genes in response to drug treatment.

2. Materials and methods

2.1. Instrumentation

Elemental analysis for C, H, and N were carried on a FISONS EA 1108 CHNS-O apparatus. The Infra-Red spectra were recorded on a Jasco spectrophotometer and the UV–Visible absorption spectra were recorded on Perkin Elmer Lambda 35 UV–Vis spectrophotometer with 10.0 mm cuvettes. A 500-MS Varian Ion Trap Mass Spectrometer was used to measure ESI-MS spectra of methanolic solutions of the complexes in the positive mode. The first derivative X-band EPR spectra of the frozen solutions (frozen in liquid nitrogen) were recorded on a Bruker ESP 300E spectrometer at 77 K. The ESP 300E spectrometer was operated at ~9.51 GHz with a frequency modulation of 100 KHz. Fluorescence measurements were carried out on a SPEX® Fluorolog spectrofluorometer (Horiba Jobin Yvon) in a FL3-11 configuration, equipped with a Xenon lamp. The instrumental response was corrected by means of a correction function provided by the manufacturer. The experiments were carried out at room temperature and are all steady-state measurements. Circular dichroism (CD) spectra were recorded at 25 °C on a Jasco J-720 spectropolarimeter with an UV–Vis (180–800 nm) photomultiplier (EXEL-308) using quartz Suprasil® CD cuvettes.

2.2. Preparation of complexes

The complexes were prepared adapting previously reported methods [19,20,24]: to a solution of glycine (ca. 1 mmol) in water, salicylaldehyde (ca. 1 mmol) was added; the mixture was stirred and heated at about ~60 °C. After ca. 15 min, a methanolic solution of the appropriate phenanthroline derivative (ca. 1 mmol) was added, followed by the addition of an equimolar amount of copper(II) acetate (ca. 1 mmol) in ~20 mL of water, and a very dark greenish solution was formed. Depending on the compound greenish/brown solids gradually deposited within about 1 to 6 h. The reaction mixtures were allowed to cool, and were filtered and washed with H_2O, ~50% methanol and diethyl ether.

2.2.1. Synthesis of Cu(Sal–Gly)(phen)

Green solid. Yield ~80%. Anal. Calcd for $C_{21}H_{15}N_3O_3Cu + 5.5\ H_2O$ (MM = 420.91 + 99.08 = 519.99), Found (Calcd) (%): C 48.41 (48.51); H 5.06 (5.04); N 7.94 (8.08). IR (KBr pellet): ν(O—H): 3200–3600, $\nu_{asym}(CO_2)$: 1647, ν(C═N) and ν(C═C): 1602,

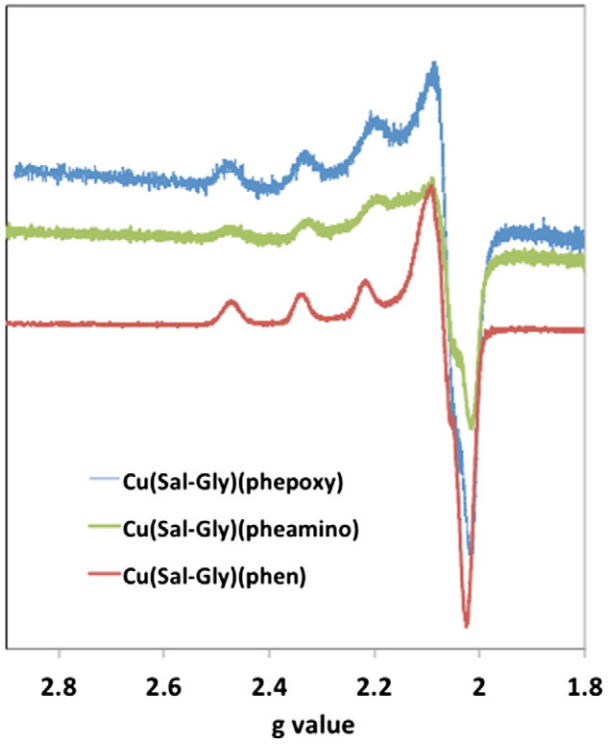

Fig. 2. First derivative X-band EPR spectra measured for frozen solutions (77 K) of the compounds. Cu(Sal-Gly)(phen) 4.0 mM in MeOH and Cu(Sal-Gly)(pheamine) and Cu(Sal-Gly)(phepoxy), 1.0 mM in DMSO.

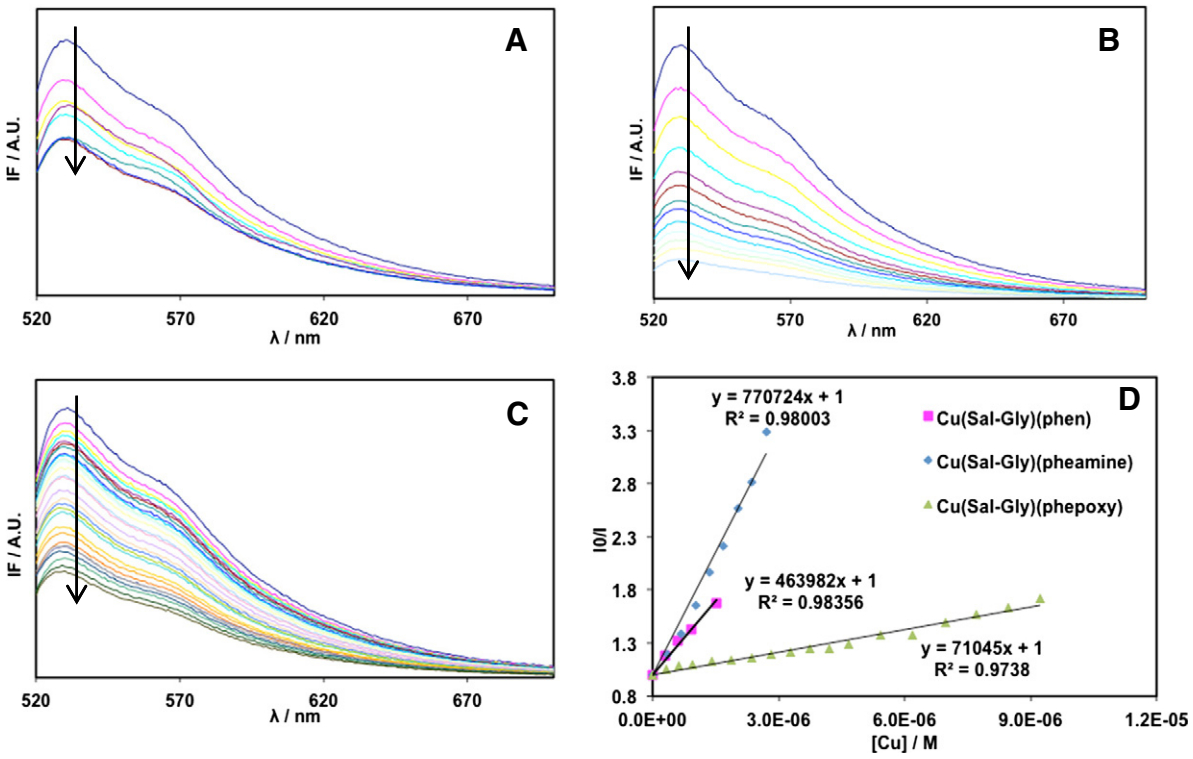

Fig. 3. Fluorescence emission spectra measured for solutions containing TO:DNA = 0.8, [CT-DNA] = 2.5 μM and increasing amounts of: A) Cu(Sal-Gly)(phen) from 0 to 2.4 μM; B) Cu(Sal-Gly)(pheamine) from 0 to 4.2 μM; and C) Cu(Sal-Gly)(phepoxy) from 0 to 18 μM. Excitation at 509 nm. Arrows indicate changes with increasing complex concentration. D) Stern–Volmer plots at 528 nm obtained from steady-state I_0/I values. The I_0/I data were corrected for inner-filter effects.

$\nu_{sym}(CO_2)$ or ν(O—Ph): 1380; C—$H_{bending}$: 775, 728 [25,26]. UV–Vis (1% DMSO and PBS): λ_{max} (nm) 242, 293, 360. Spin Hamiltonian parameters (MeOH, 4.0 mM): $g_{x,y} = 2.069$, $g_z = 2.283$, $A_{x,y} = 15.5 \times 10^{-4}\ cm^{-1}$, $A_z = 167.4 \times 10^{-4}\ cm^{-1}$.

2.2.2. Synthesis of Cu(Sal–Gly)(pheamine)

Brown solid. Yield ~60%. Anal. Calcd for $C_{21}H_{16}N_4O_3Cu + 2.5\ H_2O$ (MM = 435.92 + 45.04 = 480.96) Found (Calcd) (%): C 52.14 (52.44); H 4.10 (4.40); N 11.64 (11.65). IR (KBr pellet, cm^{-1}): ν(N—H): 3300–3500, ν(O—H): 3200–3600, $\nu_{asym}(CO_2)$: 1640, N—H_{bend}: 1622, ν(C═N) and ν(C═C): 1604, $\nu_{sym}(CO_2)$ or ν(O—Ph): 1384; C—$H_{bending}$: 766, 731 [25,26]. UV–Vis (1% DMSO and PBS): λ_{max} (nm) 265, 283, 350. Spin Hamiltonian parameters (DMSO, 1.0 mM): $g_{x,y} = 2.074$, $g_z = 2.270$, $A_{x,y} = 31.0 \times 10^{-4}\ cm^{-1}$, $A_z = 169.1 \times 10^{-4}\ cm^{-1}$.

2.2.3. Synthesis of Cu(Sal–Gly)(phepoxy)

Greenish-brown solid. Yield ~65%. Anal. Calcd for $C_{21}H_{15}N_3O_4Cu + 3.0\ H_2O$ (436.91 + 54.03 = 490.94) Found (Calcd) (%): C 51.09 (51.37); H 4.40 (4.31); N 8.87 (8.56). ν(O—H): 3200–3600, $\nu_{asym}(CO_2)$: 1644, ν(C═N): 1611, ν(C═C): 1601, $\nu_{sym}(CO_2)$ or ν(O—Ph): 1384; C—$H_{bending}$: 852, 731 [25,26]. IR (KBr pellet): $\nu_{asym}(CO_2)$: 1630 cm^{-1}, ν(C═N) and ν(C═C): 1601; $\nu_{sym}(CO_2)$ or ν(O—Ph): 1372. UV–Vis (1% DMSO and PBS): λ_{max} (nm) 273, 296, 319 (sh) 364 (sh), 420 (sh), 684. Spin Hamiltonian parameters (DMSO, 1.0 mM): $g_{x,y} = 2.078$, $g_z = 2.276$, $A_{x,y} = 18.5 \times 10^{-4}\ cm^{-1}$, $A_z = 177.8 \times 10^{-4}\ cm^{-1}$.

2.3. Calf Thymus DNA binding experiments

Millipore water was used for the preparation of TRIS and Phosphate Saline Buffer (PBS) buffers (0.10 M, pH = 7.4). DMSO from Panreac was used for the preparation of the stock solutions of the complexes. Calf Thymus DNA (CT-DNA) was purchased from Sigma (#D3664) and used as received. DNA stock solutions were prepared by dissolution in TRIS or PBS buffer. The concentration of CT-DNA was determined by UV–Vis absorbance using the molar absorption coefficient at 260 (6600 $M^{-1}\ cm^{-1}$). The UV absorbance at 260 nm and 280 nm of the CT-DNA solution gave ratios of 1.8–1.9, indicating that the DNA was sufficiently free of protein. The stock solutions of the compounds were prepared by dissolving them in DMSO and dilution in TRIS buffer; they were used within a few hours. The amount of organic solvent was kept below 1% (v/v) or 5% [for Cu(Sal-Gly)(phepoxy)]. The fluorescence experiments were done using a quartz cuvette of 1 cm path length and bandwidths of 5 nm in both excitation and emission. Titrations were done by adding increasing amounts of the complexes ([CuLL'] ~400 μM) to a solution containing thiazole orange (TO) and CT-DNA (0.8:1) ([DNA] 2.5 μM). The DNA-TO samples were excited at 509 nm and the emitted fluorescence was recorded between 520 and 700 nm. UV–Vis absorption spectra were collected in all measured systems to correct the data for reabsorption and inner filter effects [27,28]. The concentrations were selected in order to have absorbance values below 0.2 at the excitation and emission wavelengths. Blank fluorescence spectra (containing everything except the fluorophores) were measured and subtracted from each sample's emission spectra.

Circular dichroism studies were done with 3 mL solutions in quartz SUPRASIL® cuvettes of 1 cm optical path. The CT-DNA solution was prepared by dilution of the stock solution in PBS buffer and its concentration (ca. 50–60 μM) was determined in each sample by measuring the absorbance at 260 nm, prior to addition of the Cu-complexes' stock solutions in DMSO (ca. 2.0–3.0 mM) to obtain each Cu:DNA ratio. For selected samples spectra were re-measured with time, to evaluate temporal changes, which did not occur. To study the influence of the DMSO amount in the CD spectra, samples were prepared containing 0, 2.5, 5.0 and 7.5% (v/v) of DMSO. PBS buffer was used to obtain the baseline, which was subtracted from each spectrum. Spectra were collected from 200 to 350 nm with a resolution of 1 nm band width, 3 accumulations, scan speed 100 nm/min and 2 s response time.

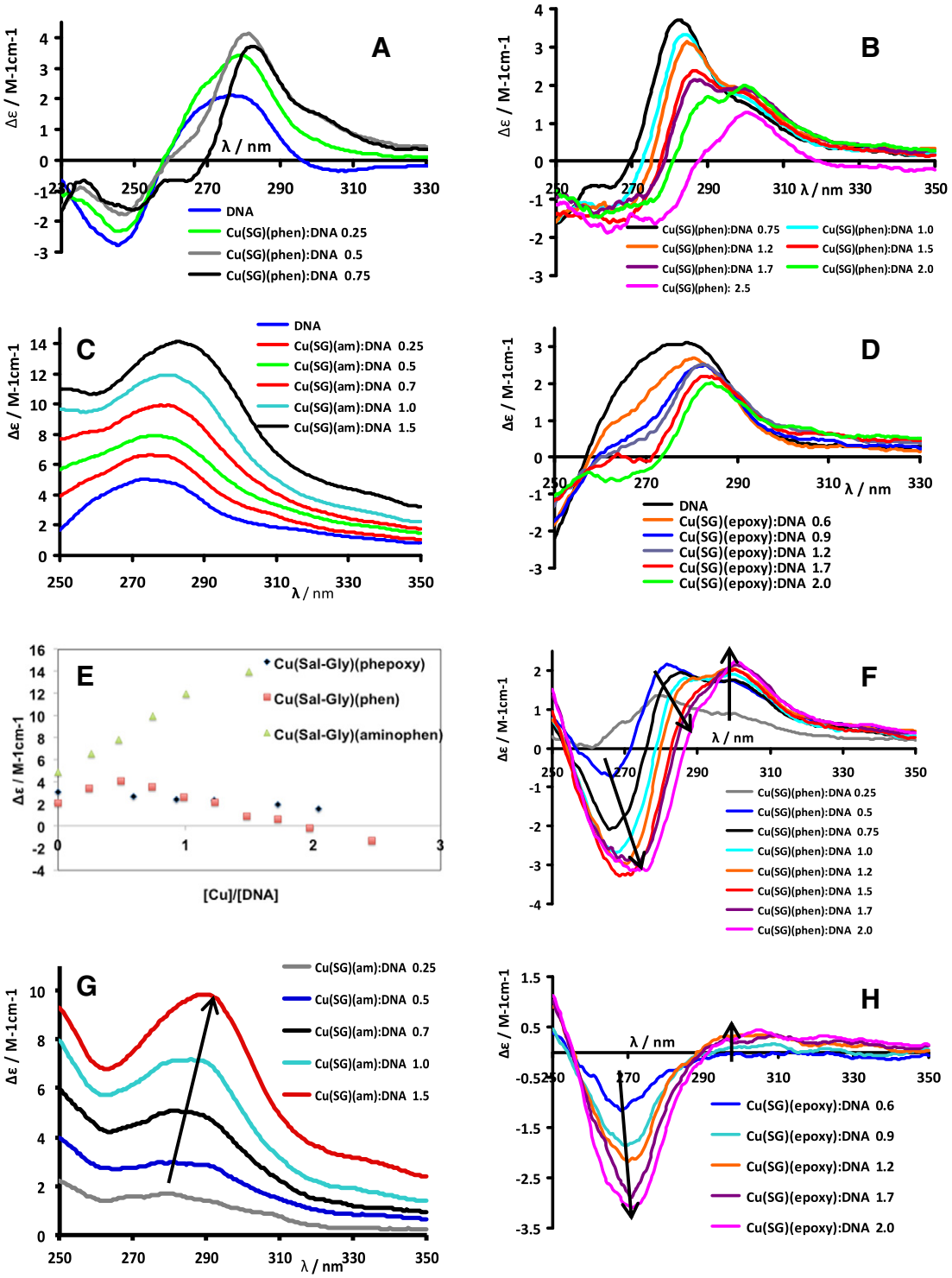

Fig. 4. Circular dichroism spectra (1 cm optical path) of CT-DNA (50–60 μM) in the absence and presence of A) and B) Cu(Sal-Gly)(phen); C) Cu(Sal-Gly)(pheamine) and D) Cu(Sal-Gly)(phepoxy) in PBS buffer (pH 7.4, 0.10 M). The molar ratios are indicated in each figure. D) Changes in the Δε observed with the molar ratios of Cu-complex to DNA. E) F) and G) Induced CD (ICD) spectra obtained by subtraction of the CD spectra of CT-DNA from each individual CD spectrum. E) Cu(Sal-Gly)(phen); F) Cu(Sal-Gly)(pheamine) and G) Cu(Sal-Gly)(phepoxy). It is assumed, but it is not necessarily correct, that by subtracting the spectrum of CT-DNA, the induced CD spectra of the complexes are obtained. However, even if not totally correct, this way of visualizing the ICD spectra helps in understanding the trends observed upon increasing the relative amount of Cu-complex present.

UV–Vis absorption titrations were done by adding aliquots of the DNA stock solution in PBS to solutions of the complexes (20 to 60 μM) in PBS (with 1% or less DMSO). Previously the complexes' stability in the aqueous media was evaluated by measuring spectral changes within 1–2 h after preparation of the solution.

2.4. Cell culturing, drug treatment and cell viability

All cancer cells (A-549, HCT-116, MDA-MB-231, HeLa and SH-SY5Y) and normal cells (HASMC1 and HASMC2) were maintained in Dulbecco's Modified Eagle Medium/F12 (DMEM/F12,

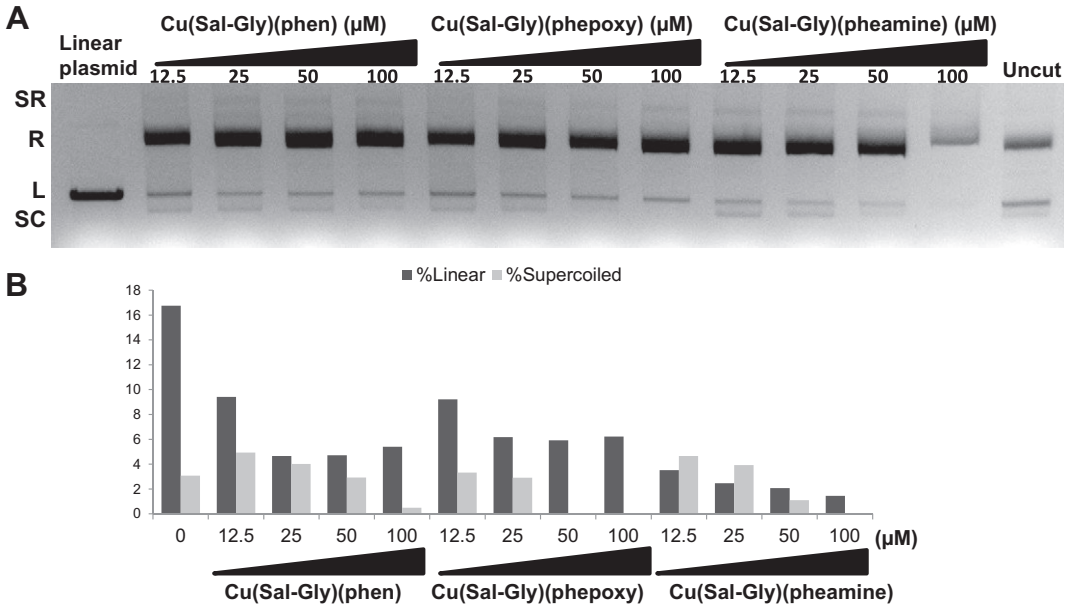

Fig. 5. Agarose gel electrophoresis of plasmid DNA incubated with the Cu-complexes. Plasmid DNA was incubated with different doses of Cu-complexes (12.5–100 μM) and the changes in the migration pattern were observed through agarose gel electrophoresis (A) and the bands were quantified using Image J software (B). Linear plasmid was obtained by *Bam*HI digestion. Addition of all Cu-complexes resulted in disappearance of the supercoiled and linear bands and increase in relaxed forms in a dose dependent manner indicating that the compounds caused single stranded DNA breaks. Treatment with 100 μM Cu(Sal-Gly)(pheamine) led to degradation of relaxed forms in addition to relaxing the double stranded plasmids, suggesting that higher doses may shear DNA. The bands are labelled as: SR: super relaxed, R: relaxed, L: linear, SC: supercoiled.

Sigma-Aldrich, #D0547) supplemented with fetal bovine serum (FBS, 5% for cancer cells and 10% for normal cells, Biochrom, #S0415) and penicillin/streptomycin (Biochrom, #A2212), and incubated at 37 °C, in 5% CO_2. For viability assays, 5–8 × 10^3 cells (~70–80% confluency depending on the cell line) were seeded in 96-well plates in regular culture medium, overnight. The following day, serial dilutions of complexes, Cu(Sal-Gly)(pheamine), Cu(Sal-Gly)(phepoxy) and Cu(Sal-Gly)(phen) (0.19–12.5 μM), were freshly prepared and added to the cells. After 24 or 72 h, cell viability was measured using MTT reagent (3-(4,5-dimethylthiazol-2-yl)-2,5-diphenyltetrazolium bromide) (Sigma, #M5655) as described before [29] and IC_{50} values were extrapolated from the

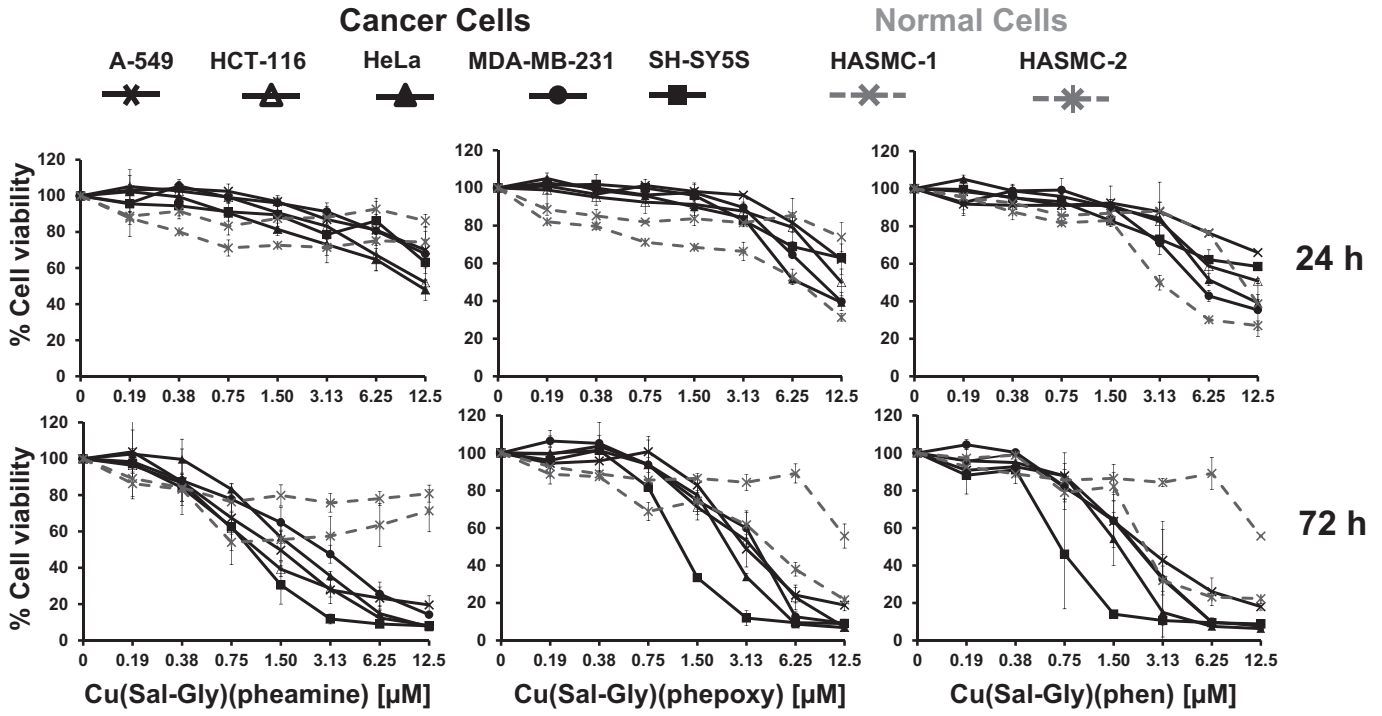

Fig. 6. Cytotoxicity of the Cu-compounds as determined by MTT analysis. Cell viability of cancer cells (Black lines: A-549, HCT-116, MDA-MB-231, HeLa, and SH-SY5Y) in comparison to non-cancer controls (Grey lines: HASMC1 and HASMC2) in response to treatment with different Cu-complexes upon increasing the dose (0–12.5 μM) at different time points (24 h, 72 h). Cell viability was measured using MTT assay. *x*-axis: concentration in μM, *y*-axis: cell viability normalized to untreated controls.

dose-response curves (Fig. 6). Sulforhodamine B (SRB) colorimetric assay was employed to verify loss in cell viability in A-549, HCT-116 and HeLa cells, as described in [30].

2.5. DNA condensation/fragmentation analysis and immunofluorescence staining

5×10^4 cells (HeLa and HCT-116) were seeded on 12 mm round cover slips and incubated overnight at 37 °C in 5% CO_2. Freshly prepared Cu-complexes (12.5 or 25 μM) were added on the cells and incubated further for 24 h. Cells were fixed in −20 °C methanol and counter stained with DAPI for nuclear morphology as described in [31]. Images were taken using fluorescence microscope (Leica DMI 6000). For immunofluorescence, cells were fixed in freshly prepared 4% paraformaldehyde for 15 min at room temperature (RT), permeabilized in 0.3% Triton X-100/PBS (1 h, RT), blocked in 0.2% gelatin (RT) and stained with γH2AX (Cell Signaling, #9718S, 1:400) or 8-oxo-Guanine (EMD Millipore, MAB3560, 1:100) antibodies overnight at 4 °C.

2.6. Plasmid DNA interaction

Plasmid DNA (100 ng, pcDNA3.1/actin-GFP, diluted in ddH_2O) was incubated with the freshly prepared Cu-complexes (12.5, 25, 50 and 100 μM) at RT for 20 h in a total reaction volume of 20 μL in ddH_2O. Linear DNA was obtained through enzymatic digestion of the plasmid DNA with *Bam*HI (MBI Fermentas). The changes in the migration pattern of the plasmid DNA were analyzed on 1% agarose gels, run at 90 V for 2.5 h. DNA bands were displayed via a UV transilluminator (UVITEC, Cambridge). Image J software was used for quantification of the bands.

2.7. Determination of caspase 3/7 activity and Annexin-V staining

2×10^5 cells (HeLa or HCT-116) were seeded in 6-well plates and cultured overnight. Cells were then treated with the Cu-complexes at the IC_{90} concentration for 24 and 48 h. At the end of the treatment, cells were washed with PBS, harvested by trypsinisation, and analyzed for the detection of early/late apoptosis and cell death mode using Annexin V/Dead Cell (kit MCH100105, Millipore, Darmstadt, Germany) and caspase 3/7 kit (MCH100108, Millipore, Darmstadt, Germany) respectively, according to the manufacturer's instructions. The live, dead, early and late apoptotic cells were counted with the Muse Cell Analyzer (Millipore, Hayward, CA, USA).

2.8. Determination of changes in MMP

The percentage of cells undergoing oxidative stress and changes in the MMP were determined by using the Muse MitoPotential kit (MCH100110, Millipore, Darmstadt, Germany) according to the manufacturer's instructions. In order to perform the assays, cells were seeded in 6-well plates and exposed to the Cu-complexes at the IC_{90} concentration for 24 and 48 h. Then, cells were washed with PBS, and collected by trypsinization. To carry out the MitoPotential assay, cells were incubated with the Muse MitoPotential working solution for 20 min at 37 °C. At the end of the incubation 7-AAD was added as a dead cell marker for an additional 5 min. Cells were analyzed by using the Muse Cell Analyzer (Millipore).

2.9. Total ROS measurement using 2′,7′–dichlorofluorescein diacetate (DCFDA)

5×10^3 cells were seeded in 96-well plates, and incubated at 37 °C in 5% CO_2. The following day, HeLa and HCT-116 cells were pretreated with 5 μM of DCFDA (dissolved in PBS, Sigma, cat # D6883) for 2 h. Following pretreatment, 5 μM of DCFDA and 0.20–12.50 μM of freshly prepared complexes, Cu(Sal-Gly)(pheamine), Cu(Sal-Gly)(phepoxy), Cu(Sal-Gly)(phen) were simultaneously added on cells. Then, plates were read on a micro-plate fluorometer (FLx800 Bio-Tek, Vermont, USA) using excitation and emission wavelengths of 485 and 535 nm, respectively. The experiment was done using three biological repeats in duplicate wells.

2.10. Measurement of GSSG/GSH

GSSG/GSH ratio was measured using Luminescence based GSH/GSSG Glo assay kit (Promega, Madison, WI, USA) following manufacturer's protocols with a slight modification. Briefly, HCT-116 and HeLa cells were seeded at a density of 5×10^3 cells per well of 96-well plate the day before drug treatment and treated with 12.5 μM of complexes for 24 h. Following treatment, medium was removed and 30 μL of Total Glutathione Lysis Reagent and/or Oxidized Glutathione Lysis Reagent was added. The plate was incubated on a plate shaker (600 rpm, RT, 5 min). An equal volume of Luciferin Generation Reagent was added and incubated in dark (RT, 30 min). Lastly, 60 μL of Luciferin Detection Reagent was added (RT, 15 min). Luminescent signal was measured using a count integration time of 1 s at luminometer (Bio-Tek, Vermont, USA). The ratio of GSSG/GSH was calculated by (GSSG RLU / 2) / (GSH RLU − GSSG RLU) equation. The experiment was replicated twice in duplicate wells.

2.11. γH2AX assay for the assessment of DNA damage using flow cytometry

HeLa and HCT-116 cells were exposed to the Cu-complexes at the IC_{90} concentration for 12 h, were centrifuged at 300 ×*g* for 5 min, washed once with PBS and fixed with the Muse Fixation Buffer, which is a component of the Muse γH2AX Activation Dual Detection (kit MCH200101, Millipore, Darmstadt, Germany) for 5 min on ice. After fixation, cells were permeabilized by ice-cold Muse Permeabilization Buffer and incubated on ice for 5 min. The cells were centrifuged (300 ×*g*, 5 min), resuspended in 45 μL 1× Assay Buffer, and incubated

Table 1
IC_{50} values deducted from the cell viability curves (Fig. 6) where the viability was in the linear range.

Cancer cells			Cancer cells		Cancer cells	
	24 h (μM)	72 h (μM)	24 h (μM)	72 h (μM)	24 h (μM)	72 h (μM)
A549	>12.50	1.93 ± 1.56	>12.50	3.32 ± 0.40	>12.50	3.58 ± 0.67
HCT 116	11.87 ± 0.66	1.79 ± 0.43	>12.50	3.84 ± 0.10	11.30 ± 0.86	3.02 ± 1.11
HeLa	10.80 ± 1.63	3.13 ± 0.51	9.16 ± 1.38	3.21 ± 0.53	7.30 ± 0.59	1.86 ± 1.34
MDA-MB-231	>12.50	3.60 ± 0.37	10.19 ± 0.49	3.70 ± 0.37	8.14 ± 0.02	3.05 ± 0.76
SHSY5Y	>12.50	1.08 ± 0.63	>12.5	1.66 ± 0.25	>12.50	0.86 ± 0.99
Non-cancer cells			Non-cancer cells		Non-cancer cells	
	24 h (μM)	72 h (μM)	24 h (μM)	72 h (μM)	24 h (μM)	72 h (μM)
HASMC1	>12.50	>12.50	>12.50	>12.50	10.81 ± 0.65	7.17 ± 0.13
HASMC2	>12.50	>12.50	7.42 ± 0.58	6.18 ± 0.34	6.31 ± 0.21	2.47 ± 0.32

Table 2
Significance of data. Cell viability between cancer cells and non-cancer controls was compared following 24 or 72 h of drug exposure. The area under cell viability curves was calculated and the statistical analysis was performed using independent samples *t*-test. A *p*-value below 0.01 was considered to be significant.

p value (AUC, *t*-test)	Cu(Sal-Gly) (pheamine)	Cu(Sal-Gly) (phepoxy)	Cu(Sal-Gly) (phen)
24 h	$p = 0.387$	$p = 0.562$	$p = 0.484$
72 h	$p = 0.001$	$p = 0.047$	$p = 0.018$

with the mixture of 2.5 μL of antiphospho-Histone H2AX and 2.5 μL of anti-Histone H2AX, PECy5 (30 min, dark, at RT). At the end of the incubation, cells were resuspended in 100 μL of 1 × Assay Buffer, centrifuged (300 × *g*, 5 min), and resuspended in 150 μL of 1 × Assay Buffer. The data were acquired on the Muse Cell Analyzer (Millipore, Hayward, CA, USA).

2.12. RNA isolation and real time qPCR

3×10^5 cells were seeded in 35 mm plates, and incubated under cell culture conditions. The following day, 3.13 μM of freshly prepared Cu(Sal-Gly)(pheamine) was added on the cells and incubated for 48 h. Total RNA was isolated similarly to previously described before [32] using Nucleospin RNAII kit (Macherey-Nagel, Germany), and was measured using NanoDrop™ 1000 Spectrophotometer, Celbio. 1000 ng total RNA was used for cDNA synthesis. Three housekeeping genes (GAPDH, HPRT1, YWHAZ) were used for relative quantification of the target genes.

3. Results and discussion

3.1. Syntheses and characterization of complexes

The Cu^{II}-complexes were prepared using a common synthetic procedure by reaction of a stoichiometric amount of the corresponding metal salt with the corresponding ligand and co-ligand. The resulting compounds precipitated as green (or brown) microcrystalline solids and were characterized by elemental analysis, UV–Vis, FTIR and EPR spectroscopies, and by ESI-MS. Cu(Sal-Gly)(phen) was previously reported [19,20,24], but Cu(Sal-Gly)(pheamine) and Cu(Sal-Gly)(phepoxy) are novel complexes.

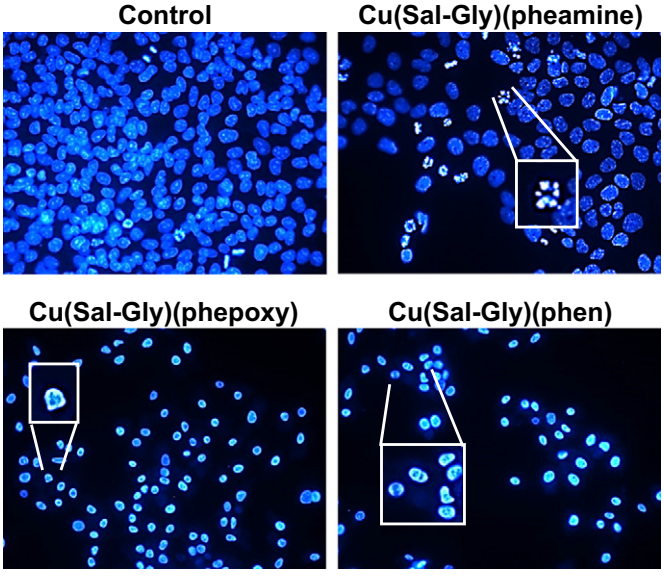

Fig. 7. Change in the nuclear morphology of cells in response to Cu-complexes. HeLa cells treated with 12.5 μM of Cu-complexes are shown in the figure. Insets indicate enlarged views of selected cells exhibiting these features. HeLa cells displayed typical features of apoptosis such as fragmentation and condensation. Note that the nuclei appear smaller and more intense (condensed) and in smaller pieces (fragmented) in treated samples with fewer cells per frame compared to untreated control.

Fig. 1 depicts the structural formulae of the compounds Cu(Sal-Gly)(phen) (MW: 420.91), Cu(Sal-Gly)(pheamine) (MW: 435.92) and Cu(Sal-Gly)(phepoxy) (MW: 436.91), which are under analysis in this study. The compounds were synthesized as described in Materials and methods section and were obtained in reasonable yields (≥60%), all containing water molecules. The ESI-MS spectra of Cu(Sal-Gly)(phepoxy) measured in the positive mode showed a peak at *m/z* 423.18 with 100% abundance and the Cu isotopic pattern. This peak may be assigned to the Cu-complex upon deoxygenation of the epoxide, the heterocyclic ligand being 5,6-dihydro-1,10-phenanthroline. For Cu(Sal-Gly)(pheamine), the most abundant peak at *m/z* 453.18 was assigned to $[ML_1L_2 + NH_4]^+$ (theoretical: 453.08). For Cu(Sal-Gly)(phen) the most abundant peak appeared at *m/z* 423.15, which was the same observed for Cu(Sal-Gly)(phepoxy). Another one was observed at *m/z* 840.48 (30%) that we assign to $[2(ML_1L_2) + H]^+$ (theoretical: 841.08).

In general, the Cu^{II} and the previously reported $V^{IV}O$-complexes [19] exhibit comparable spectroscopic features, suggesting that they have similar molecular structures. For $V^{IV}O$(Sal-L-Ala)(H_2O) the IR spectrum was calculated by DFT methodologies [26] and the $\nu_{asym}(CO_2)$, ν(C═N) and $\nu_{sym}(CO_2)$ stretches appeared at ca. 1640, 1600 and 1380 cm^{-1}, respectively. ν(C═C) also showed up at ca. 1600 cm^{-1}. All three Cu^{II}-compounds had bands at 1640–1650, 1600–1610 and 1380–1385 cm^{-1} that were assigned accordingly.

The isotropic electronic absorption spectra of the complexes (see examples included in Fig. 1 in ref [30]) depict strong intraligand bands at 230–250 and at 270–300 nm and an intense band at 375–385 nm, frequently assigned to azomethine π–π* from the Schiff base, [26,33] as well as weak d-d bands. TD-DFT (time-dependent density functional theory) calculations for [$V^{IV}O$(Sal-L-Ala)(H_2O)] [26] allowed assignment of these bands to a predominantly LMCT (ligand to metal charge transfer) band ($PhO^- \rightarrow V$), specifically a transition from π* (phenol) to a π V—N bond, also spread over benzene π* and the d_{xz} orbital, thus we favor an equivalent assignment for the present set of compounds.

The 1st derivative EPR spectra measured from DMSO solutions [or MeOH for Cu(Sal-Gly)(phen)] frozen at 77 K (Fig. 2) show axial symmetry with a more intense absorption at higher field. The spin Hamiltonian parameters obtained by simulation of the experimental spectra are included in the Materials and methods section. No superhyperfine coupling with the nitrogen donors could be observed, due to the low bandwidth resolution, which is common in solvents with high viscosity such as DMSO.

Peisach and Blumberg compiled experimental g_z and A_z values obtained from a wide range of model Cu^{II}-compounds and constructed a g_z/A_z plot [34]. This representation allowed the establishment of correlations between geometry, donor group and experimental g_z and A_z data obtained from EPR spectra. Sakaguchi and Addison [35] published an updated version of this plot, and introduced another empirical relation known as the tetrahedral distortion index, which is obtained by dividing g_z for A_z (in cm^{-1}). Values ranging from 100 to 135 cm indicate a square-planar geometry with minimal distortion and the larger this index, the greater the extent of the tetrahedral distortion. For the present complexes the representation of the (g_z, A_z) data in the g_z/A_z plot fall between the values typical of N_2O_2 and O_4 binding sets, and the g_z/A_z values are 136, 134 and 128 for Cu(Sal-Gly)(phen), Cu(Sal-Gly)(pheamine) and Cu(Sal-Gly)(phepoxy), respectively. This suggests that the N_3O_2 (or N_3O_3, if a water molecule is also coordinated to the Cu^{II}-center) probably corresponds to a square-pyramidal (or elongated octahedral, if H_2O is coordinated) geometry, with relatively weakly bound axial donor atom(s).

To evaluate the stability of the complexes in organic solvents EPR spectra were recorded with time. Spectra are included in Fig. 2 in ref [30], and show that all Cu^{II}-complexes are reasonably stable since only

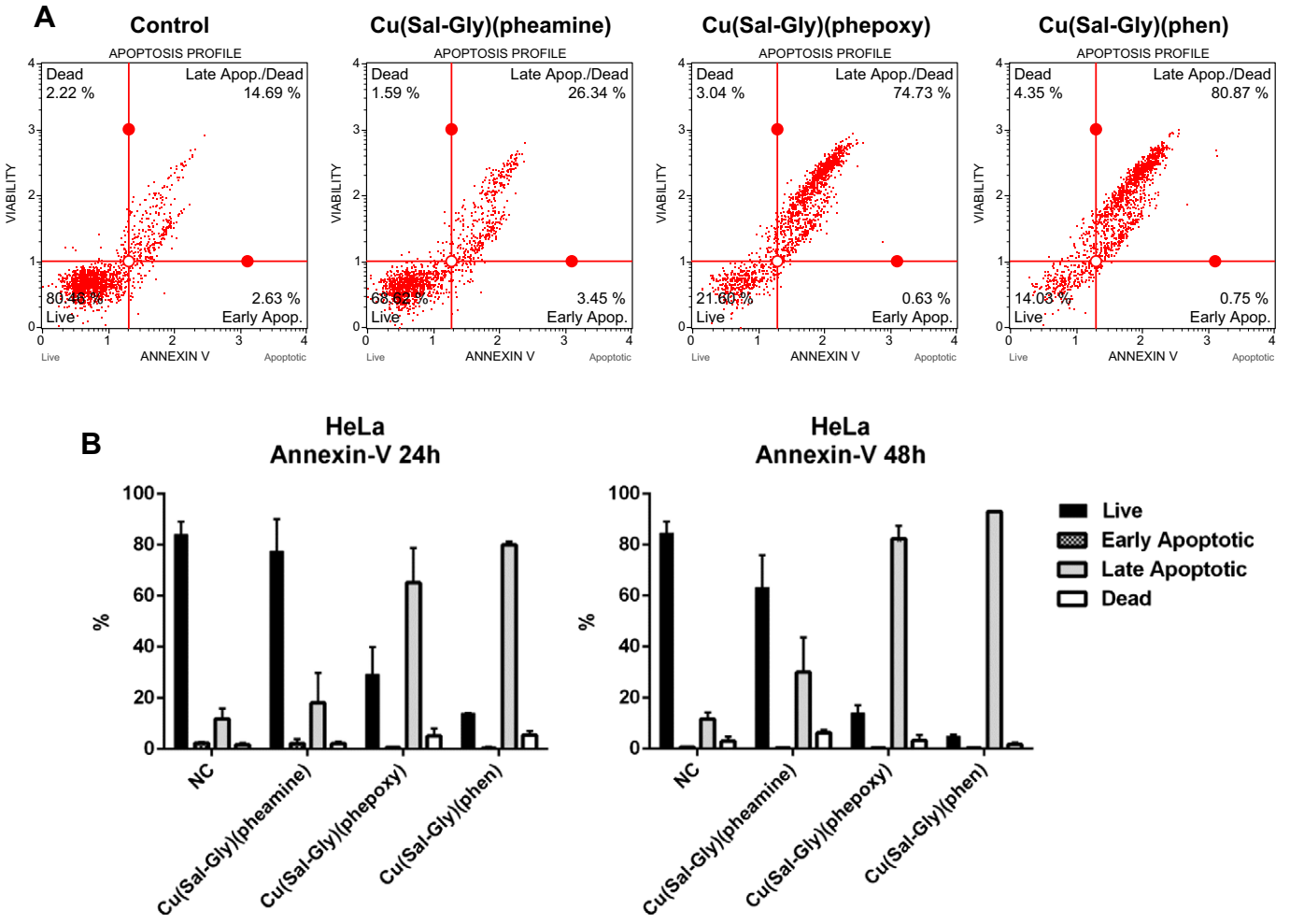

Fig. 8. Cu-complexes induce apoptosis in HeLa cells as determined by Annexin V/PI staining. HeLa cells were treated with the Cu-complexes and were stained with Annexin V/dead cell marker and counted with a flow cytometer as described in Materials and methods. Representative plots for HeLa cells following 24 h drug exposure are shown in the figure (A). The graphs represent averages from 2 independent experiments from 24 h of exposure (left graph) and 48 h of exposure (right graph), where 10,000 cells were scored (B). *x*-axis: % cells, *y*-axis: name of the drug, NC: negative control, mock treated cells.

a small decrease with time is observed in the intensity of the EPR spectra. The stability of the complexes in PBS (pH 7.4, containing ca. 1% DMSO) was also evaluated by UV–Vis isotropic absorption. Data show reasonable stability for the Cu^{II}-compounds derived from phen and phepoxy for at least 1 h, since only minor changes are observed in the spectra within this time frame (Fig. S3). For Cu(Sal-Gly)(pheamine) slightly more significant changes were observed in the 250–290 nm range and isosbestic points are detected.

3.2. DNA binding experiments

3.2.1. Competitive binding studies

Competitive binding of drugs to DNA provides information regarding the DNA binding affinity. Ethidium bromide (EB) is widely used in competitive binding studies involving DNA to probe binding by intercalation. The enhancement of EB fluorescence through binding to dsDNA is ca. 20-fold and varies with base pair's sequence. Thiazole orange (TO) exhibits a different excitation and emission fluorescence (509 and 527 nm, respectively) and displays a higher, less sequence dependent affinity for DNA, generating a higher fluorescence enhancement upon binding to duplex DNA (50–2000 vs 20-fold for EB) [36]. For these reasons, as well as the higher toxicity of EB, TO was chosen as the intercalator in the fluorescence competition titrations. The study started by evaluating the best DNA:TO ratio to maximize the TO fluorescence emission, which under the experimental conditions - TRIS buffer 0.10 M, pH 7.4, 2.5 μM CT-DNA – was a ratio TO:DNA = 0.8.

All studied complexes showed very low intensity fluorescence when excited at 509 nm, and the corresponding fluorescence spectra were subtracted from the DNA-TO-CuL spectra. Fig. 3 shows fluorescence emission spectra measured for the three systems containing TO:DNA = 0.8, by addition of increasing amounts of each complex, indicated in the caption. In all cases, fluorescence quenching was observed – ca. 35, 85 and 62% – for the Cu-complexes containing phen, pheamine and phepoxy, respectively, indicating that they were able to compete with TO for the same binding sites, or interact with DNA at different sites.

The quenching data was analyzed with the Stern–Volmer equation,

$$I_0/I = K_{SV}[Q] + 1$$

where I_0 is the emission intensity in the absence of the quencher, I is the emission intensity in the presence of the quencher, K_{SV} is the quenching Stern-Volmer constant, and [Q] is quencher concentration. The K_{SV} value is obtained as the slope from the plot of I_0/I versus [Q]. The Stern-Volmer plots obtained after correction for inner filter effects and reabsorption [27,28] are shown in Fig. 3. The K_{SV} constants obtained were: 4.6×10^5 and 7.7×10^5 M^{-1} for Cu(Sal-Gly)(phen) and Cu(Sal-Gly)(pheamine), respectively, and 7.1×10^4 M^{-1}, one order of magnitude lower, for Cu(Sal-Gly)(phepoxy).

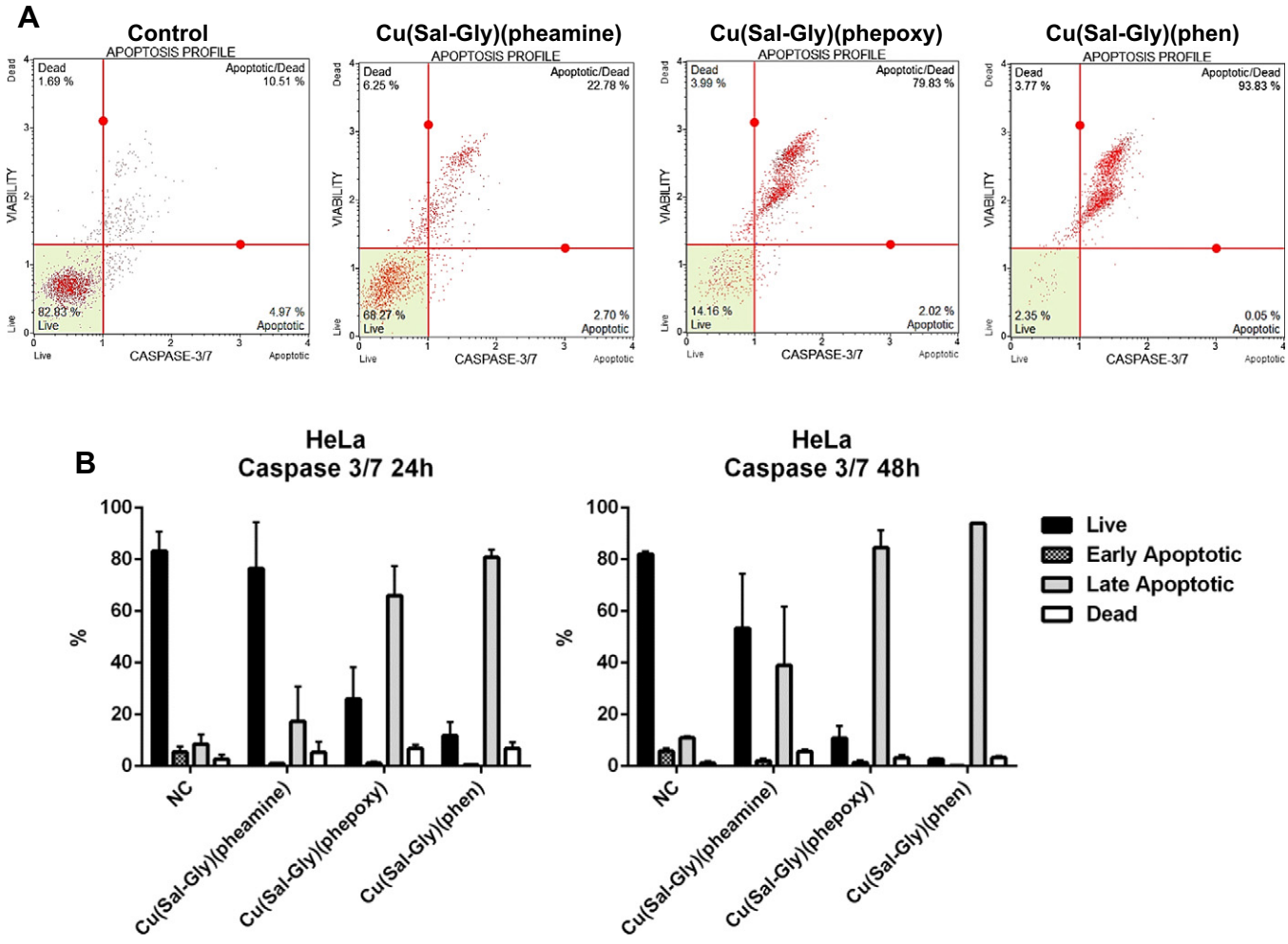

Fig. 9. Induction of caspase 3/7 activity in response to Cu-complexes. HeLa cells were treated with the Cu-complexes and were stained using caspase 3/7 kit and counted with a flow cytometer as described in Materials and methods. Representative plots for HeLa cells following 48 h drug exposure are shown in the figure (A). The graphs represent averages from 2 independent experiments from 24 h of exposure (left graph) and 48 h of exposure (right graph), where 10,000 cells were scored (B). *x*-axis: % cells, *y*-axis: name of the drug, NC: negative control, mock treated cells.

The binding constant (K_{app}) values can be obtained using the following equation:

$$K_{TO}[TO] = K_{app}[Q]$$

in which the quencher concentration [Q] has the value at 50% reduction of the fluorescence intensity, $K_{TO} = 1.9 \times 10^6\ M^{-1}$ [37] and [TO] is the TO concentration used in each assay (ca. 2.0 μM). Since in the system with Cu(Sal-Gly)(phen) the fluorescence quenching saturated at ca. 35%, the [Q] at 50% quenching was extrapolated. The following values were obtained for the binding constants: ~1.7×10^6, $2.4(8) \times 10^6$ and $3.2(3) \times 10^5\ M^{-1}$, for Cu(Sal-Gly)(phen), Cu(Sal-Gly)(pheamine) and Cu(Sal-Gly)(phepoxy), respectively. We can conclude that the phen and pheamine complexes have similar affinity for CT-DNA, with the presence of the amino group enhancing the affinity in Cu(Sal-Gly)(pheamine), possibly due to electrostatic and hydrogen bonding interactions between the charged amino group ($NH3+$) and phosphate (and sugar) moieties of DNA. The complex with phepoxy as co-ligand shows much lower affinity.

3.2.2. Circular dichroism (CD) binding studies

DNA is chiral due to the chiral sugars and sugar–phosphate backbone, and thus, produces a characteristic CD spectrum in the 200–300 nm range. Changes in this spectral region are useful to detect DNA conformational changes, damage and/or cleavage. Even for non-chiral complexes, their association with the right-handed DNA helix, besides possibly affecting the 3D arrangement of the CT-DNA helix, thus its CD spectrum, may also give rise to induced CD spectra (ICD) in the range where the complexes present absorption bands. CT-DNA in PBS buffer showed a spectrum characteristic for right-handed B-form consisting of a positive band centered at ~275 nm, mainly due to base stacking and a negative band at ~245 nm, a result of right-handed helicity [38].

Fig. 4 shows the CD spectra measured for solutions containing ca. 50–60 μM of CT-DNA and different amounts of the Cu-complexes. Addition of the complexes changed quite significantly both the intensity and the shape of the DNA UV-bands, and thus we can definitely infer that these compounds are able to interact with CT-DNA. Since DMSO was used to dissolve the complexes, its effect on DNA was also evaluated. Upon observation of Fig. 3 in ref [30], it can be concluded that DMSO affects the band up to ~245 nm even for 2.5% v/v, but not much the bands for $\lambda > 250$ nm; this is why the spectra depicted in Fig. 4 were cut at 250 nm. However, even with 7% v/v DMSO only minor changes were observed in the ~275 nm positive band. Nonetheless, the % DMSO in the studies was always kept below 5%, and considerations will be made only from effects observed above 250 nm.

Fig. 4 depicts the changes observed in the positive band, which is mainly due to base stacking in CT-DNA. From the data presented, we can speculate that the changes observed in the CD spectra for the complexes containing phen and phepoxy ligands are rather similar: above

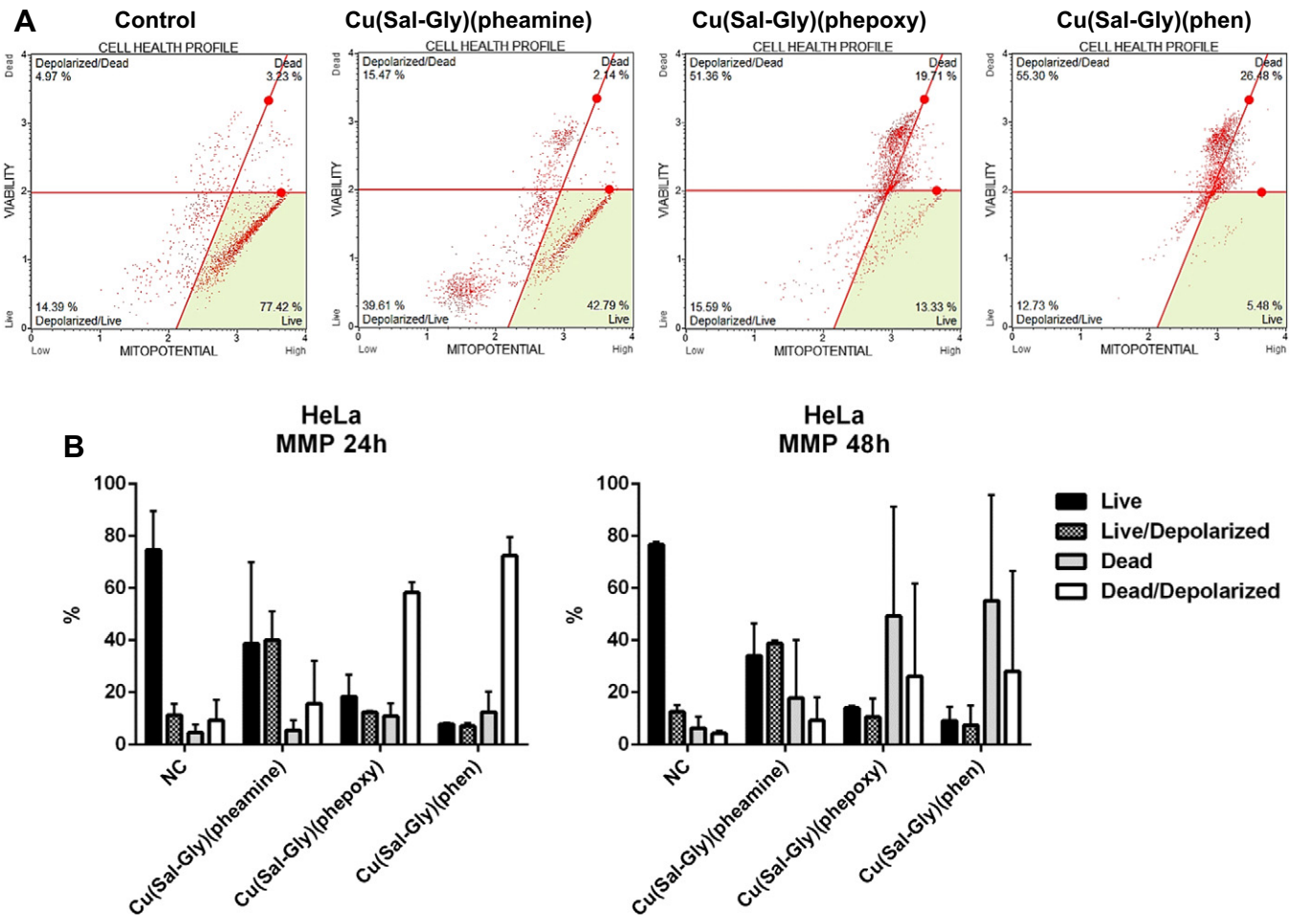

Fig. 10. Change in MMP in response to Cu-complexes. HeLa cells were treated with the Cu-complexes and were stained using MitoPotential kit and counted with a flow cytometer as described in Materials and methods. Representative plots for HeLa cells following 48 h drug exposure are shown in the figure (A). The graphs represent averages from 2 independent experiments from 24 h of exposure (left graph) and 48 h of exposure (right graph), where 10,000 cells were scored (B). *x*-axis: % cells, *y*-axis: name of the drug, NC: negative control, mock treated cells.

the ratio [Cu]/[DNA] of ~0.5 the positive bands loose intensity, while for the pheamine complex the intensity of this band increases steadily. This indicates that the interaction of Cu(Sal-Gly)(pheamine) with CT-DNA is much stronger; probably the amino moiety is partly protonated this allowing a stronger interaction with the phosphate groups of DNA and also with the chiral sugar moieties.

In order to get further insight into the changes occurring in the systems and taking into consideration: i) the presence of isodichroic points in some systems and ii) the fact that the measured CD spectrum is the weighted sum of the spectrum of each individual chiral species in solution, the ICD spectra were evaluated by subtraction of the DNA spectrum, since in solution we may have the chiral DNA, and one or more chiral DNA-copper adducts. The resulting ICD spectra are depicted in Fig. 4.

Interpretation of the data is not straightforward; however, a few considerations can be made. In the Cu(Sal-Gly)(phepoxy) system (Fig. 4H) only one species seemed to be present up to a ratio of Cu:DNA of 2:1, since only one negative signal centered at ca. 270 nm is observed.

In the Cu(Sal-Gly)(phen) system (Fig. 4F), a similar band was observed, however, another chiral species may be contributing to the total CD signal since there were isodichroic points (between 290 and 300 nm) and other bands present. A total of 3 bands could be observed. The spectrum with ratio Complex:DNA = 0.5 showed bands at 266 (−), 282 (+) and 299 (+) nm. Increasing the amount of the Cu-complex: i) increased the intensity of the 266 nm (−) band that shifted to 273 nm; decreased the intensity and shifted the maximum of the 282 nm band to 290 nm; iii) the band at 299 slightly increased in intensity. Globally, the magnitude of the ICD bands was similar in both the Cu(Sal-Gly)(phen) and Cu(Sal-Gly)(phepoxy) systems.

The ICD bands observed in the system containing Cu(Sal-Gly)(pheamine) (Fig. 4G) was considerably different from those for the other two complexes, both in form and magnitude. It has been reported that intercalators generally exhibit small ICD signals ($<10\ M^{-1}\ cm^{-1}$), with larger ICD signals being indicative of groove-binding interactions [38]. As mentioned above, the presence of the amino group (a significant fraction of it as NH_3^+) in the phenanthroline ligand allows the involvement of this group in electrostatic interactions with negatively-charged phosphate groups. Hydrogen bonds with other moieties, e.g. sugar OH groups, may also be relevant. Therefore the binding may involve grove binding and/or hydrogen bonding. Nonetheless, intercalation cannot be excluded and probably several types of binding are involved, resulting in higher binding affinity for this complex when compared to the others, as was observed in the fluorescence competition studies.

3.2.3. UV–Vis isotropic absorption spectral studies

Attempts were made to determine DNA binding constants from UV–Vis absorption titrations, however, the small changes occurring with time in the complexes' solutions diluted in buffer precluded the use of this technique for this purpose. Nonetheless, qualitative observations can be made (Fig. 4 in Ref. [30]): i) a faster decrease in the

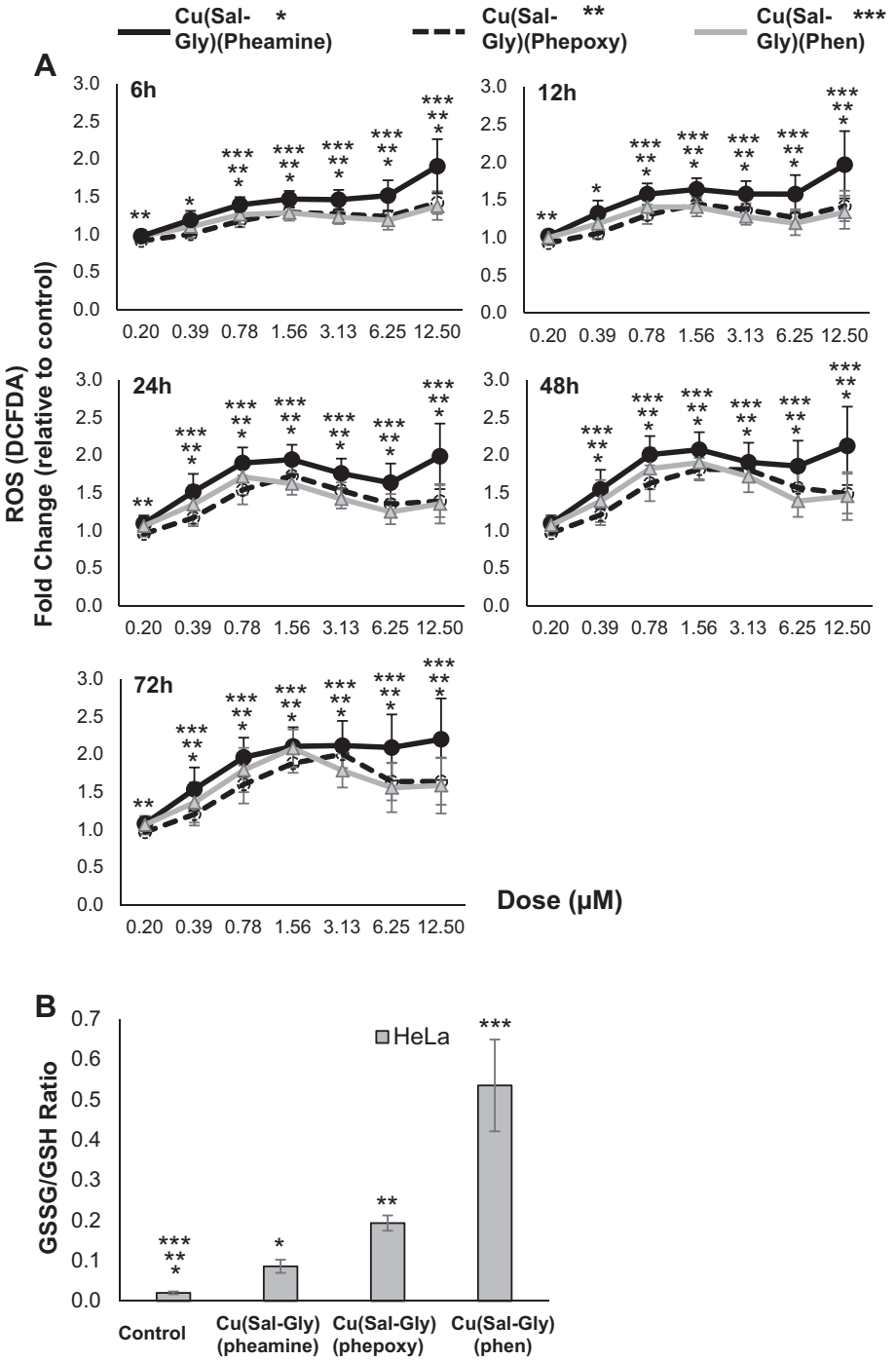

Fig. 11. Increase in ROS in response to Cu-complexes. (A) Cells were pretreated with DCFDA with the indicated doses of Cu-complexes for 6–72 h and ROS was measured as described in Materials and methods. Averages from at least three replicates from HeLa cells are shown in the graphs. *y*-axis: fold increase in DCFDA staining of cells relative to untreated controls, *x*-axis: concentration of Cu-complexes (μM). Asterisks denote significant change compared to untreated controls (Paired samples *t*-test, $p < 0.05$). (*: Cu(Sal-Gly)(pheamine), **: Cu(Sal-Gly)(phepoxy), ***: Cu(Sal-Gly)(phen).) (B) HeLa cells were treated with 12.5 μM of the Cu-complexes and lysed 24 h post-incubation. The cellular GSSG/GSH (oxidized/reduced forms of glutathione) levels were measured, and a significant increase in oxidation was observed with all three Cu-complexes. Significance is indicated by asterisks (Paired samples *t*-test, $p < 0.05$).

absorbance values at 267 nm for solutions containing Cu(Sal-Gly)(phen) and CT-DNA 1:1 can be observed, when compared to the solution containing the complex alone (ca. ~5% decrease vs. 8.5%); ii) a decrease in the intensity of the intraligand bands at 256 and 278 nm when increasing amounts of DNA are added to a solution containing Cu(Sal-Gly)(pheamine) and iii) a small decrease in the intensity of the band at 273 nm upon addition of CT-DNA to Cu(Sal-Gly)(phepoxy). All these observations are consistent with the binding of the complexes to DNA.

3.2.4. DNA cleavage activity

In order to test the interaction of the complexes with DNA, 12.5, 25, 50 or 100 μM of the compounds were incubated with plasmid DNA (pcDNA3.1 actin) for 16 h, and the plasmid DNA was run on agarose

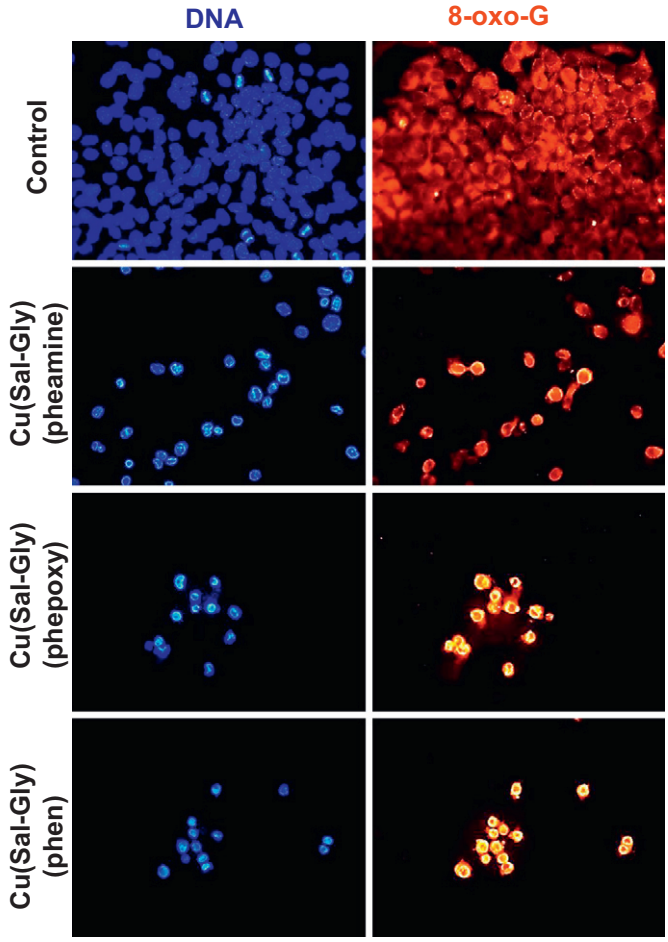

Fig. 12. Oxidative DNA damage in response to Cu-complexes as determined by 8-oxo-G staining. HeLa cells were treated with the 12.5 μM of Cu-complexes for 24 h and were stained for DNA (blue) and 8-oxo-guanine (red), the most common lesion in response to oxidative stress. 8-oxo-G staining was increased upon treatment with all Cu-complexes.

gels (Fig. 5A). Linear form was visualized by enzymatic digestion (*Bam*HI) of the plasmid DNA. As expected, uncut plasmid (last lane) showed three major bands, representing the supercoiled, linear and relaxed (plasmid DNA nicked on a single strand) forms of DNA. The intensity of the bands was quantified from the gel images and the analysis showed that increasing doses of all three compounds lead to disappearance of the supercoiled band and a subsequent increase in the relaxed form (Fig. 5B). The difference was most pronounced with Cu(Sal-Gly)(pheamine), where both the linear and supercoiled bands were lost at the highest concentration. This result suggests that the complexes induce DNA breaks, which were mostly single stranded as shown by relaxation of the supercoiled form. When two single stranded breaks (SSB) were close together, they probably led to a double stranded break (DSB), hence disappearance of the linear and even relaxed forms due to shearing of DNA as seen in the lane of 100 μM treatment of Cu(Sal-Gly)(pheamine).

3.3. Cytotoxicity of the complexes

The potency of the compounds was investigated on various cancer cell lines of different origins such as lung (A-549), colon (HCT-116), breast (MDA-MB-231), cervix (HeLa), and neural tissue (SH-SY5Y) in comparison to non-cancer controls (HASMC1 and HASMC2). Cells were exposed to 0–12.5 μM of the complexes for 24 h or 72 h, and cell viability was determined using MTT assay, a colorimetric assay based on metabolic activity (Fig. 6). The cytotoxicity was confirmed using another method on a subset of cancer cell lines (A-549, HCT-116 and HeLa) using SRB analysis, which measures cellular protein content to evaluate viability (Fig. 5 in Ref. [30]). Our results indicate that all three compounds were cytotoxic on all cell lines tested, and the effect was more pronounced by 72 h compared to 24 h (Fig. 6, top panel versus bottom panel). The half maximal effective doses were determined from the dose response curves, and the IC_{50} values were calculated (Table 1). In order to assess specificity towards cancer cells, cell viability between cancer cells and non-cancer controls was compared via area under curve analysis (Table 2). Area under curve was selected as some of the calculated IC_{50} values were above the highest tested concentration (12.5 μM). Interestingly, while all compounds were effective in killing cancer cells, Cu(Sal-Gly)(pheamine) was significantly more potent on cancer cells (independent samples *t*-test, $p < 0.01$). As specificity is one of the foremost properties expected from an ideal anticancer drug, Cu(Sal-Gly)(pheamine) appears to be the most promising compound among the derivatives reported here.

3.4. Mode of cell death

3.4.1. Nuclear morphology

One of the first steps in investigating the cytotoxic activity of novel complexes involves determination of the mean of cell death, and understanding whether the process occurs through programmed pathways. Hence, a series of experiments were set to thoroughly assess how the cells die in response to these Cu-complexes. HeLa cells were treated with 12.5 μM of Cu(Sal-Gly)(pheamine), Cu(Sal-Gly)(phepoxy) or Cu(Sal-Gly)(phen), and the chromosomal morphology was examined. In accordance with our cell viability analysis, there was a great reduction in the number of cells per field after exposure to all drugs (Fig. 7). The results were replicated in HCT-116 cells (Fig. 6 in ref [30]). Furthermore, typical characteristics of apoptosis, signified by pyknotic and fragmented nuclei were observed, indicating apoptosis as the mean of cell death (Fig. 7, Fig. 6 insets in ref [30]).

3.4.2. Annexin V/7-AAD analysis

Annexin V is a well-established marker to investigate apoptosis even at early stages [39]. Flow cytometry analysis of HeLa cells stained with Annexin V/7-AAD revealed an increase in phosphatidylserine externalization both after 24 h and 48 h, with all drugs under investigation (Fig. 8). The increase was most evident following treatment with Cu(Sal-Gly)(phen), and least for Cu(Sal-Gly)(pheamine) exposure after 24 h, which were further elevated at 48 h (Fig. 8B). Therefore, cells responded differently to Cu(Sal-Gly)(pheamine) both in terms of time and level of increase in Annexin V, potentially allowing an explanation for the specificity of Cu(Sal-Gly)(pheamine).

For all drugs under investigation, Annexin V positive cells were mostly in the late apoptotic quadrant, which could imply that the time for early apoptosis might have been missed by 24 h. However, this result did not change even when earlier time points were taken (data not shown). Hence, it appears that cells quickly proceeded to later stages of apoptosis, leading to only a slight increase in the early apoptotic quadrant and a larger elevation in the late apoptotic cells. Similar results were obtained when another cell line (HCT-116) was used to confirm these findings (Fig. 7 in ref [30]).

3.4.3. Caspase 3/7 activity

One of the essential steps during apoptosis is activation of executioner caspases [40,41]. Hence, caspase 3/7 activity was monitored 24 h and 48 h following drug exposure, and analyzed via flow cytometry (Fig. 9). The activity was examined in combination with a dead cell dye (7AAD) that provided information on membrane integrity, distinguishing cells that are apoptotic/live and apoptotic/dead (Fig. 9A, bottom right and top right quadrants). Elevated levels of caspase 3/7 activity were observed in response to exposure to all three complexes, once again with highest increase after treatment with Cu(Sal-Gly)(phen) and lowest with Cu(Sal-Gly)(pheamine) (Fig. 9B). The results were repeated in

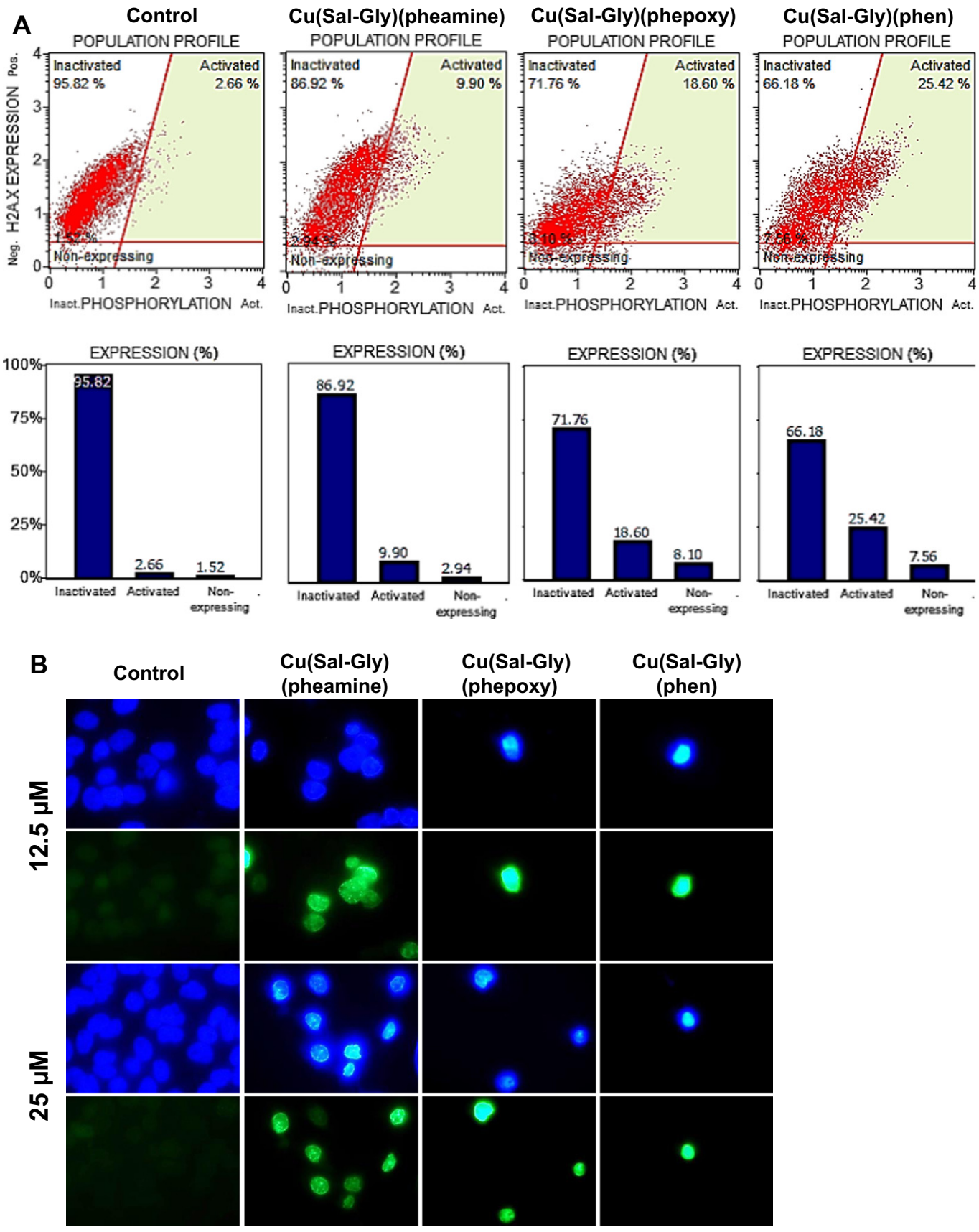

Fig. 13. Cu-complexes induce DNA double strand breaks. (A) HeLa cells were treated with IC_{90} values of the Cu-complexes for 12 h, and were stained with both anti-phospho-Histone H2AX (Ser139) and anti-Histone H2AX antibodies, and quantified using a flow cytometer. Non-expressing quadrant indicates cells that do not express H2AX antigen, inactivated quadrant indicates the cells expressing H2AX without phosphorylation and activated quadrant indicates the γH2AX phosphorylated cells. The quantification of results is shown in the graphs. (B) In order to visually determine γH2AX positivity, HeLa cells were treated with 12.5 and 25 µM of the Cu-complexes, stained for γH2AX and observed under the fluorescence microscope. Images were taken using 100× magnification.

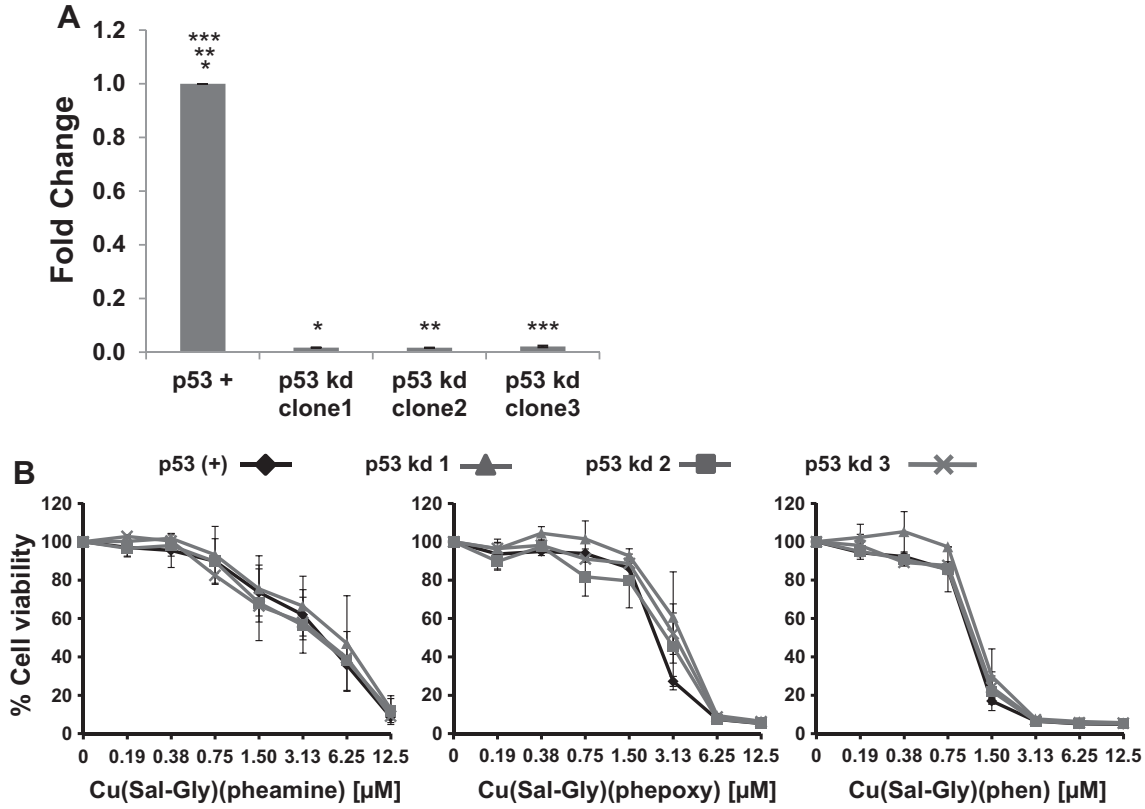

Fig. 14. Induction of cell death in p53 deficient cells. To determine if the p53 status of cells affects cell death induced by the Cu-complexes, three stable p53 knock-down cells were generated from p53 positive HeLa cells. (A) RT-qPCR analysis showing the efficiency of knock down in each clone used in this study. (B) Cell viability in response to Cu-complexes following 72 h treatment in p53 positive (p53(+)) parental cells or p53 knock down (p53 kd) clones. It is concluded that Cu-complexes can induce cell death in p53 deficient cells.

HCT-116 cells with similar outcomes (Fig. 8 in ref [30]). Therefore, our data support apoptotic pathways that are dependent on caspase activity.

3.4.4. Mitochondrial membrane potential (MMP)

Depolarization of the mitochondrial membrane is considered as one of the initial and irreversible steps during the process of apoptosis, albeit not necessarily obligate for apoptosis induction to occur [42]. In order to investigate if apoptosis induced by our Cu^{II}-complexes involved disruption of mitochondrial membrane integrity, MMP was monitored via flow cytometry in combination with a live/dead cell marker. Hence, four populations of cells were counted as live, depolarized/live, depolarized/dead, and dead cells (Fig. 10A, Fig. 9A in ref [30]). Consistent with our previous observations, we detected loss of MMP with all three compounds suggesting apoptotic pathways. While the shift from live cells was mostly to depolarized/live population in response to Cu(Sal-Gly)(pheamine) (Fig. 10B, Fig. 9 in ref [30]), the shift was towards the depolarized/dead by 24 h, and then towards the dead population following treatment with Cu(Sal-Gly)(phepoxy) and Cu(Sal-Gly)(phen). Hence, the degree of the molecular changes that occur in response to Cu(Sal-Gly)(pheamine) seemed to be milder than with the other derivatives, which could explain specificity for cancer cells. Interestingly, despite the lowest level of increase in Annexin V, caspase activity and MMP; cell death was similar in comparison to other derivatives (Fig. 11 and Table 2), which could indicate other forms of cell death in addition to apoptosis following Cu(Sal-Gly)(pheamine) treatment.

3.5. Oxidative DNA damage

Many metal based compounds depend on their redox chemistry and their ability to activate oxygen to induce DNA damage/cleavage [43]. In order to assess the oxidative stress in cells in response to the present Cu-complexes, radical formation was quantitatively measured using DCFDA, a well-characterized agent for the detection of ROS in cell populations. Both HeLa and HCT-116 cells showed an increase in intracellular ROS formation in a dose dependent manner following treatment with all three drugs compared to vehicle treated controls (Fig. 11A, Fig. 10A in ref [30]) (Paired samples *t*-test, $p < 0.05$ at indicated doses). The increase in ROS started as early as 6 h after treatment and was detectable throughout the treatment at all time points tested (6, 12, 24, 48, 72 h). Hence, it appears that the Cu-complexes under investigation may induce oxidative stress in cells. The increase in ROS was the

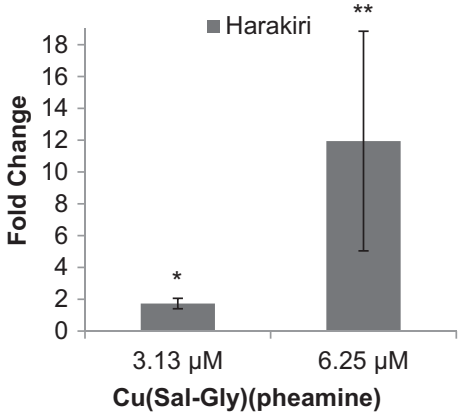

Fig. 15. Gene expression changes in response to Cu(Sal-Gly)(pheamine) treatment. The expression of Harakiri was upregulated following in a dose dependent manner following Cu(Sal-Gly)(pheamine) treatment. *x*-axis: concentration of Cu(Sal-Gly)(pheamine), *y*-axis: fold change relative to untreated controls. Asterisks indicate significance. (Paired samples *t*-test, *: $p = 0.000$, **: $p = 0.012$.)

most evident following Cu(Sal-Gly)(pheamine) in both cell lines tested. Therefore, Cu(Sal-Gly)(pheamine) appears to act differently from the other derivatives, which is another property that may help in understanding the observed specificity.

To assess the cellular effects of ROS overproduction, we examined oxidation of glutathione (GSH), which prevents cell damage caused by ROS through generation of GSSG. Upon exposure to elevated oxidative stress, cells accumulate GSSG and the ratio of GSSG to GSH increases. Only one time point (24 h) and concentration (12.5 μM) was selected for this analysis. As expected, GSSG/GSH ratio was significantly increased upon exposure to all Cu-complexes compared to vehicle treated controls in both HeLa (Fig. 11B) and HCT-116 cells (Fig. 10B in ref [30]) (Paired samples *t*-test, $p < 0.05$ where indicated by the asterisks). The degree of increase was different in the two cell lines probably reflecting differences in their genetic background. This result further supported our previous finding for increased oxidative stress in response to Cu-complexes.

As DNA is sensitive to oxidation, the possible damage on DNA by these complexes was tested via staining for 8-oxo-guanine, which is the most abundant lesion due to determine the extent of cellular oxidative stress [44]. There is a clear induction in the fluorescence intensity following all drug treatments in both HeLa and HCT-116 cells (Fig. 12 and Fig. 11 in ref [30]). Hence, all three complexes induced formation of ROS, which possibly triggered DNA oxidation. The damage might be mediated by diffusible species and oxidative chemistry at a distance, by specific and tight non-covalent interactions of the Cu-complexes with the DNA, or by formation of DNA adducts of the Cu-complexes [43]. Indeed, the present studies may grant the base for further experiments to test which of these mechanisms take place in the Cu-induced DNA lesions in cells (Fig. 12).

3.6. Double stranded DNA breaks in response to drug treatment

Our in vitro plasmid ligation assay provides preliminary information on how the complexes might be interacting with DNA; and the complexes appear to induce SSBs, which may eventually lead to DSBs, if the nicks are close enough (Fig. 5). To test this hypothesis in cell culture, both HeLa and HCT-116 cells were treated with the Cu-complexes, and stained for γH2AX, which is a sensitive and well-established marker to evaluate formation of DSBs [45]. All complexes activated H2AX phosphorylation, although the percentage in the increase for γH2AX expression varied (Fig. 13, Fig. 12 in ref [30]). The expression was quantitatively evaluated using flow cytometry (Fig. 13A, Fig. 12A in ref [30]), and also qualitatively through immunofluorescence microscopy (Fig. 13B, Fig. 12B in ref [30]) in line with each other in both cell lines. Therefore, all three complexes appeared to induce DSBs in cell culture, which might have been due to increased oxidative species.

3.7. Role of p53 in drug induced cell death

As p53 is considered to be the guardian of the genome, we wished to determine if the p53 status of the cells had any effect on the cytotoxicity of the compounds. For this purpose, we used HeLa cells, which have wild type p53 ([46], RIKEN Biosource Center DNA Bank, and our own observations), and three clones of HeLa cells that were stably transfected with a lentiviral shRNA towards p53. The efficiency of knockdown in the clones used in this study is shown in Fig. 14A (independent samples *t*-test, $p = 0.000$ between the p53 + and silenced cells for all clones). Our results showed that cell viability was similar in HeLa cells irrespective of their p53 status in response to all three complexes after 72 h of drug exposure (Fig. 14B). This result indicated that the pathways in response to these compounds either did not involve p53 mediated cell death, or that other pathways may become activated to compensate for the absence of p53 to induce cell death. Hence, the complexes appear to be equally effective in p53 deficient cancers. As p53 is mutated in approximately 50% of the cancers [47], the Cu-complexes used in this study are expected to be potent even in the p53 deficient cancer cells.

3.8. Molecular changes triggered by drug exposure

Compared to platinum compounds, not much is known about the molecular basis of the mechanism of action on Cu-complexes. Non-platinum active compounds are likely to exert a different mechanism of action, which may make them potential drugs in poor chemosensitive or resistant human cancers, and display broader spectrum [9]. Based on current literature, Cu-complexes can exert their cytotoxic effect through DNA damage [3,48,49], via inhibition of topoisomerases [50–52] or inhibition of the proteasome pathway [7,53,54]. Since our observations indicated oxidative stress induced DNA damage as the mechanism of action, and apoptosis as the mode of cell death, we developed a custom RT-qPCR array consisting of 80 genes, which cover DNA damage response pathway, oxidative stress genes as well as apoptotic genes to be able to understand which molecules were active during drug induced cell death. Cu(Sal-Gly)(pheamine) was selected for further investigation, as among the present Cu-complexes under evaluation, it is the most specific towards cancer cells (*t*-test, $p < 0.01$). HeLa cells were treated with 3.13 μM of Cu(Sal-Gly)(pheamine) for 48 h and total RNA was isolated. The dose and time point was selected based on visual inspection of cells in combination with cell viability analysis, where the cells were affected but not dead. The array was run in duplicate using two different extracts and genes that showed significant >1.5-fold up/down regulation were re-tested in a third extract. The arithmetic average of three housekeeping genes (YWHAZ, HPRT and GAPDH) was used for normalization. The average fold change, standard deviations and *p*-values are given in Table 1 in ref [30]. Our analysis revealed that only one out of 80 genes (Harakiri) was upregulated consistently and significantly (Paired samples *t*-test, $p = 0.000$). The expression was reevaluated using 6.25 μM drug treatment, and it was found to be further elevated, suggesting that the increase was dose dependent (Fig. 15, Paired samples *t*-test, $p = 0.012$). As Harakiri has been shown to induce cell death through its interactions and inhibition of Bcl-2 and Bcl-XL [55], the intrinsic apoptotic pathways seem to be activated in response to Cu(Sal-Gly)(pheamine).

4. Conclusions

Three copper(II) mixed-ligand complexes, Cu(Sal-Gly)(phen), Cu(Sal-Gly)(pheamine) and Cu(Sal-Gly)(phepoxy), containing the Schiff-base derived from the reaction of salicylaldehyde and glycine as one of the ligands and 1,10-phenanthroline and derivatives as co-ligand are synthesized and characterized. The compounds are isolated as green/brown solids, also containing water molecules; their spectroscopic properties suggest they correspond to N_3O_2 (or N_3O_3, if a water molecule is coordinated) binding sets with slightly distorted square-pyramidal (or elongated octahedral, if a water molecule is coordinated) geometry.

All compounds interact with CT-DNA, this being clearly shown by circular dichroism and fluorimetric measurements. From fluorimetry the binding constants were evaluated as ~1.7×10^6, 2.5×10^6 and 3.2×10^5 M^{-1}, for Cu(Sal-Gly)(phen), Cu(Sal-Gly)(pheamine) and Cu(Sal-Gly)(phepoxy), respectively. CD spectra in the range 250–350 nm depict significant changes as the Cu/DNA molar ratios increase, particularly in the case of Cu(Sal-Gly)(pheamine), possibly because in this complex the presence of the NH_3^+ in the pheamine co-ligand allows additional interactions with the phosphate and sugar (chiral) moieties.

Besides binding to CT-DNA, the three Cu-compounds studied induce DNA damage as determined by cleavage of supercoiled DNA in vitro and induction of 8-oxo-guanidine and γH2AX staining in cells. The complexes also induced ROS in cells, which are likely to be responsible for the observed DNA damage, which may eventually lead to cell death. While all three complexes were cytotoxic, especially after 72 h, one of

the compounds, Cu(Sal-Gly)(pheamine), showed specificity towards cancer cells. Our analysis also showed that phenotypes associated with Cu(Sal-Gly)(pheamine) were slightly different from the other two compounds under analysis, such as the time required to induce phosphatidylserine translocation (Annexin V staining), caspase 3/7 activity or mitochondrial membrane depolarization (compare induction between 24 h and 48 h) and the level of induction for these parameters. In all cases, Cu(Sal-Gly)(pheamine) showed the mildest phenotypes while retaining similar levels of cell death. Perhaps, the damage induced by Cu(Sal-Gly)(pheamine) can be tolerated by normal cells, yet is enough to kill cancer cells, potentially explaining the specificity of this compound. In order to ameliorate cancer cell specificity, we are currently investigating the use of nanocarrier systems for the controlled and targeted delivery of this compound to cancer cells.

Since Cu(Sal-Gly)(pheamine) was the most specific complex, it was further tested for molecular changes in response to drug treatment using a custom designed RT-qPCR array, where potential genes involved in oxidative stress, DNA damage or apoptosis were studied. Only one gene, Harakiri, which is an activator of apoptosis, was found to be upregulated (>1.5-fold) significantly in response to Cu(Sal-Gly)(pheamine). As Harakiri is a part of intrinsic apoptotic pathway [55], this finding is well in accordance with DNA damage induced cell death response. Interestingly, although there was a drastic increase in caspase 3/7 activity in response to treatment with Cu(Sal-Gly)(pheamine), there was no significant increase in the mRNA expression. Hence, the increase in activity appears to be post-transcriptionally, indicating a more rapid response such as through cleavage of caspase 3 and/or 7. Consistent with p53 independent cell death, there was no significant difference in the mRNA expression of p53. Indeed, we cannot exclude the possibility that p53 might still be involved in Cu(Sal-Gly)(pheamine) induced cell death through post-transcriptional events such as oligomerization or other post translational modifications; and that its absence could be tolerated by redundant proteins.

Copper being an essential element, Cu^{II}-compounds are expectedly less toxic than those based on metals such as Pt. Thus, globally the presently studied complexes may be considered potentially useful anticancer agents with activity in cancer cells even with deficient p53 status.

Conflicts of interest

The authors declare no conflict of interest.

Transparency document

The Transparency document associated with this article can be found, in the online version.

Acknowledgements

The authors thank the financial support from the Portuguese Fundação para a Ciência e a Tecnologia (project UID/QUI/00100/2013), program Investigador FCT, TUBITAK Internal Funding, and the IST-UTL Center of the Portuguese Mass Spectrometry Networks (REM2013, RECI/QEQ-QIN/0189/2012). We also thank Dr. Somnath Roy for the initial set-up of synthesis of Cu(Sal-Gly)(pheamine) and Cu(Sal-Gly)(phepoxy) compounds.

Appendix A. Supplementary data

Supplementary data to this article can be found online at http://dx.doi.org/10.1016/j.bbagen.2016.10.014.

References

[1] T.C. Johnstone, G.Y. Park, S.J. Lippard, Understanding and improving platinum anticancer drugs—phenanthriplatin, Anticancer Res. 34 (2014) 471–476.
[2] C.X. Zhang, S.J. Lippard, New metal complexes as potential therapeutics, Curr. Opin. Chem. Biol. 7 (2003) 481–489.
[3] C. Santini, M. Pellei, V. Gandin, M. Porchia, F. Tisato, C. Marzano, Advances in copper complexes as anticancer agents, Chem. Rev. 114 (2014) 815–862.
[4] Z.L. Harris, J.D. Gitlin, Genetic and molecular basis for copper toxicity, Am. J. Clin. Nutr. 63 (1996) 836s–841s.
[5] L. Ruiz-Azuara, M.E. Bravo-Gomez, Copper compounds in cancer chemotherapy, Curr. Med. Chem. 17 (2010) 3606–3615.
[6] S. Tardito, L. Marchio, Copper compounds in anticancer strategies, Curr. Med. Chem. 16 (2009) 1325–1348.
[7] K.G. Daniel, P. Gupta, R.H. Harbach, W.C. Guida, Q.P. Dou, Organic copper complexes as a new class of proteasome inhibitors and apoptosis inducers in human cancer cells, Biochem. Pharmacol. 67 (2004) 1139–1151.
[8] A. Gupte, R.J. Mumper, Elevated copper and oxidative stress in cancer cells as a target for cancer treatment, Cancer Treat. Rev. 35 (2009) 32–46.
[9] C. Marzano, M. Pellei, F. Tisato, C. Santini, Copper complexes as anticancer agents, Anti Cancer Agents Med. Chem. 9 (2009) 185–211.
[10] F. Tisato, C. Marzano, M. Porchia, M. Pellei, C. Santini, Copper in diseases and treatments, and copper-based anticancer strategies, Med. Res. Rev. 30 (2010) 708–749.
[11] R. Huang, A. Wallqvist, D.G. Covell, Anticancer metal compounds in NCI's tumor-screening database: putative mode of action, Biochem. Pharmacol. 69 (2005) 1009–1039.
[12] M.E. Letelier, A.M. Lepe, M. Faundez, J. Salazar, R. Marin, P. Aracena, H. Speisky, Possible mechanisms underlying copper-induced damage in biological membranes leading to cellular toxicity, Chem. Biol. Interact. 151 (2005) 71–82.
[13] F. Carvallo-Chaigneau, C. Trejo-Solis, C. Gomez-Ruiz, E. Rodriguez-Aguilera, L. Macias-Rosales, E. Cortes-Barberena, C. Cedillo-Pelaez, I. Gracia-Mora, L. Ruiz-Azuara, V. Madrid-Marina, F. Constantino-Casas, Casiopeina III-ia induces apoptosis in HCT-15 cells in vitro through caspase-dependent mechanisms and has antitumor effect in vivo, Biometals 21 (2008) 17–28.
[14] C. Trejo-Solis, G. Palencia, S. Zuniga, A. Rodriguez-Ropon, L. Osorio-Rico, S.T. Luvia, I. Gracia-Mora, L. Marquez-Rosado, A. Sanchez, M.E. Moreno-Garcia, A. Cruz, M.E. Bravo-Gomez, L. Ruiz-Ramirez, S. Rodriguez-Enriquez, J. Sotelo, Cas IIgly induces apoptosis in glioma C6 cells in vitro and in vivo through caspase-dependent and caspase-independent mechanisms, Neoplasia (New York, N.Y.) 7 (2005) 563–574.
[15] M. Devereux, M. McCann, D. O'Shea, M. O'Connor, E. Kiely, V. McKee, D. Naughton, A. Fisher, A. Kellett, M. Walsh, D. Egan, C. Deegan, Synthesis, superoxide dismutase mimetic and anticancer activities of metal complexes of 2,2-dimethylpentanedioic acid(2dmepdaH$_2$) and 3,3-dimethylpentanedioic acid(3dmepdaH$_2$): X-ray crystal structures of [Cu(3dmepda)(bipy)]$_2$·6H$_2$O and [Cu(2dmepda)(bipy)(EtOH)]$_2$·4EtOH (bipy = 2,2′bipyridine), Bioinorg. Chem. Appl. (2006) 80283.
[16] C. Deegan, B. Coyle, M. McCann, M. Devereux, D.A. Egan, In vitro anti-tumour effect of 1,10-phenanthroline-5,6-dione (phendione), [Cu(phendione)$_3$](ClO$_4$)$_2$·4H$_2$O and [Ag(phendione)$_2$]ClO$_4$ using human epithelial cell lines, Chem. Biol. Interact. 164 (2006) 115–125.
[17] C. Deegan, M. McCann, M. Devereux, B. Coyle, D.A. Egan, In vitro cancer chemotherapeutic activity of 1,10-phenanthroline (phen), [Ag$_2$(phen)$_3$(mal)]x2H$_2$O, [Cu(phen)$_2$(mal)]x2H$_2$O and [Mn(phen)$_2$(mal)]x2H$_2$O (malH$_2$ = malonic acid) using human cancer cells, Cancer Lett. 247 (2007) 224–233.
[18] M.E. Bravo-Gomez, J.C. Garcia-Ramos, I. Gracia-Mora, L. Ruiz-Azuara, Antiproliferative activity and QSAR study of copper(II) mixed chelate [Cu(N-N)(acetylacetonato)]NO$_3$ and [Cu(N-N)(glycinato)]NO$_3$ complexes, (Casiopeinas), J. Inorg. Biochem. 103 (2009) 299–309.
[19] I. Correia, S. Roy, C.P. Matos, S. Borovic, N. Butenko, I. Cavaco, F. Marques, J. Lorenzo, A. Rodriguez, V. Moreno, J.C. Pessoa, Vanadium(IV) and copper(II) complexes of salicylaldimines and aromatic heterocycles: cytotoxicity, DNA binding and DNA cleavage properties, J. Inorg. Biochem. 147 (2015) 134–146.
[20] A.K. Patra, M. Nethaji, A.R. Chakravarty, Synthesis, crystal structure, DNA binding and photo-induced DNA cleavage activity of (*S*-methyl-L-cysteine)copper(II) complexes of heterocyclic bases, J. Inorg. Biochem. 101 (2007) 233–244.
[21] A.K. Patra, S. Roy, A.R. Chakravarty, Synthesis, crystal structures, DNA binding and cleavage activity of L-glutamine copper(II) complexes of heterocyclic bases, Inorg. Chim. Acta 362 (2009) 1591–1599.
[22] R. Rao, A.K. Patra, P.R. Chetana, DNA binding and oxidative cleavage activity of ternary (L-proline)copper(II) complexes of heterocyclic bases, Polyhedron 26 (2007) 5331–5338.
[23] S. Gama, I. Rodrigues, F. Marques, E. Palma, I. Correia, M.F.N.N. Carvalho, J.C. Pessoa, A. Cruz, S. Mendo, I.C. Santos, F. Mendes, I. Santos, A. Paulo, New ternary bipyridine-terpyridine copper(II) complexes as self-activating chemical nucleases, RSC Adv. 4 (2014) 61363–61377.
[24] P.A.N. Reddy, M. Nethaji, A.R. Chakravarty, Synthesis, crystal structures and properties of ternary copper(II) complexes having 2,2′-bipyridine and α-amino acid salicylaldiminates as models for the type-2 sites in copper oxidases, Inorg. Chim. Acta 337 (2002) 450–458.
[25] D.H. Williams, I. Fleming, Spectroscopic Methods in Organic Chemistry, McGraw-Hill, London, 1995.
[26] J. Costa Pessoa, M.J. Calhorda, I. Cavaco, I. Correia, M.T. Duarte, V. Felix, R.T. Henriques, M.F.M. Piedade, I. Tomaz, Molecular modelling studies of N-salicylideneamino acidato complexes of oxovanadium(IV). Molecular and crystal structure of a new dinuclear LOV^{IV}-O-V^{V}OL mixed valence complex, J. Chem. Soc. Dalton Trans. (2002) 4407–4415.

[27] A. Coutinho, M. Prieto, Ribonuclease T1 and alcohol dehydrogenase fluorescence quenching by acrylamide: a laboratory experiment for undergraduate students, J. Chem. Educ. 70 (1993) 425.
[28] B. Valeur, M.N. Berberan-Santos, Molecular Fluorescence, 2 ed Wiley-VCH, Weinheim, 2012.
[29] B. Cevatemre, F. Ari, M. Sarimahmut, A.Y. Oral, E. Dere, O. Kacar, Z. Adiguzel, C. Acilan, E. Ulukaya, Combination of fenretinide and indole-3-carbinol results in synergistic cytotoxic activity inducing apoptosis against human breast cancer cells in vitro, Anti-Cancer Drugs 24 (2013) 577–586.
[30] C. Acilan, Z. Adiguzel, B. Cevatemre, D. Karakas, E. Ulukaya, N. Ribeiro, I. Correia, J.C. Pessoa, Validation Data Supporting the Characterization of Novel Copper Complexes as Anticancer Agents, Data in Brief, 2016 (*submitted*).
[31] C. Acilan, M. Serhatli, O. Kacar, Z. Adiguzel, A. Tuncer, M. Hayran, K. Baysal, Smooth muscle cells isolated from thoracic aortic aneurysms exhibit increased genomic damage, but similar tendency for apoptosis, DNA Cell Biol. 31 (2012) 1523–1534.
[32] Z. Adiguzel, A.T. Baykal, O. Kacar, V.T. Yilmaz, E. Ulukaya, C. Acilan, Biochemical and proteomic analysis of a potential anticancer agent: palladium(II) Saccharinate complex of terpyridine acting through double strand break formation, J. Proteome Res. 13 (2014) 5240–5249.
[33] J.C. Pessoa, M.J. Calhorda, I. Cavaco, P.J. Costa, I. Correia, D. Costa, L.F. Vilas-Boas, V. Felix, R.D. Gillard, R.T. Henriques, R. Wiggins, *N*-Salicylideneamino acidato complexes of oxovanadium(IV). The cysteine and penicillamine complexes, Dalton Trans. (2004) 2855–2866.
[34] J. Peisach, W.E. Blumberg, Structural implications derived from the analysis of electron paramagnetic resonance spectra of natural and artificial copper proteins, Arch. Biochem. Biophys. 165 (1974) 691–708.
[35] U. Sakaguchi, A.W. Addison, Spectroscopic and redox studies of some copper(II) complexes with biomimetic donor atoms: implications for protein copper centres, J. Chem. Soc. Dalton Trans. (1979) 600–608.
[36] J. Nygren, N. Svanvik, M. Kubista, The interactions between the fluorescent dye thiazole orange and DNA, Biopolymers 46 (1998) 39–51.
[37] J.T. Petty, J.A. Bordelon, M.E. Robertson, Thermodynamic characterization of the association of cyanine dyes with DNA, J. Phys. Chem. B 104 (2000) 2561–2569.
[38] N.C. Garbett, P.A. Ragazzon, J.B. Chaires, Circular dichroism to determine binding mode and affinity of ligand-DNA interactions, Nat. Protoc. 2 (2007) 3166–3172.
[39] G. Zhang, V. Gurtu, S.R. Kain, G. Yan, Early detection of apoptosis using a fluorescent conjugate of annexin V, BioTechniques 23 (1997) 525–531.
[40] E. Ulukaya, C. Acilan, Y. Yilmaz, Apoptosis: why and how does it occur in biology? Cell Biochem. Funct. 29 (2011) 468–480.
[41] E. Ulukaya, C. Acilan, F. Ari, E. Ikitimur, Y. Yilmaz, A glance at the methods for detection of apoptosis qualitatively and quantitatively, Turk. J. Biochem. 36 (2011) 261–269.
[42] J.D. Ly, D.R. Grubb, A. Lawen, The mitochondrial membrane potential (deltapsi(m)) in apoptosis; an update, Apoptosis 8 (2003) 115–128.
[43] G. Pratviel, Oxidative DNA damage mediated by transition metal ions and their complexes, Met. Ions Life Sci. 10 (2012) 201–216.
[44] P.H. Aguiar, C. Furtado, B.M. Repoles, G.A. Ribeiro, I.C. Mendes, E.F. Peloso, F.R. Gadelha, A.M. Macedo, G.R. Franco, S.D. Pena, S.M. Teixeira, L.Q. Vieira, A.A. Guarneri, L.O. Andrade, C.R. Machado, Oxidative stress and DNA lesions: the role of 8-oxoguanine lesions in *Trypanosoma cruzi* cell viability, PLoS Negl. Trop. Dis. 7 (2013) e2279.
[45] V. Turinetto, C. Giachino, Multiple facets of histone variant H2AX: a DNA double-strand-break marker with several biological functions, Nucleic Acids Res. 43 (2015) 2489–2498.
[46] L.Q. Jia, M. Osada, C. Ishioka, M. Gamo, S. Ikawa, T. Suzuki, H. Shimodaira, T. Niitani, T. Kudo, M. Akiyama, N. Kimura, M. Matsuo, H. Mizusawa, N. Tanaka, H. Koyama, M. Namba, R. Kanamaru, T. Kuroki, Screening the p53 status of human cell lines using a yeast functional assay, Mol. Carcinog. 19 (1997) 243–253.
[47] M. Hollstein, D. Sidransky, B. Vogelstein, C.C. Harris, p53 mutations in human cancers, Sci. 253 (1991) 49–53.
[48] D. Montagner, V. Gandin, C. Marzano, A. Erxleben, DNA damage and induction of apoptosis in pancreatic cancer cells by a new dinuclear bis(triazacyclonane) copper complex, J. Inorg. Biochem. 145 (2015) 101–107.
[49] Z. Molphy, C. Slator, C. Chatgilialoglu, A. Kellett, DNA oxidation profiles of copper phenanthrene chemical nucleases, Front. Chem. 3 (2015) 28.
[50] T. Huang, C. Li, X. Sun, Z. Zhu, Y. Fu, Y. Liu, Y. Yuan, S. Li, C. Li, The antitumor mechanism of di-2-pyridylketone 2-pyridine carboxylic acid hydrazone and its copper complex in ROS generation and topoisomerase inhibition, and hydrazone involvement in oxygen-catalytic iron mobilization, Int. J. Oncol. 47 (2015) 1854–1862.
[51] S.T. Chew, K.M. Lo, S.K. Lee, M.P. Heng, W.Y. Teoh, K.S. Sim, K.W. Tan, Copper complexes with phosphonium containing hydrazone ligand: topoisomerase inhibition and cytotoxicity study, Eur. J. Med. Chem. 76 (2014) 397–407.
[52] F. Bacher, E. Enyedy, N.V. Nagy, A. Rockenbauer, G.M. Bognar, R. Trondl, M.S. Novak, E. Klapproth, T. Kiss, V.B. Arion, Copper(II) complexes with highly water-soluble L- and D-proline-thiosemicarbazone conjugates as potential inhibitors of Topoisomerase IIalpha, Inorg. Chem. 52 (2013) 8895–8908.
[53] Z. Skrott, B. Cvek, Diethyldithiocarbamate complex with copper: the mechanism of action in cancer cells, Mini-Rev. Med. Chem. 12 (2012) 1184–1192.
[54] F. Wang, P. Jiao, M. Qi, M. Frezza, Q.P. Dou, B. Yan, Turning tumor-promoting copper into an anti-cancer weapon via high-throughput chemistry, Curr. Med. Chem. 17 (2010) 2685–2698.
[55] N. Inohara, L. Ding, S. Chen, G. Nunez, Harakiri, a novel regulator of cell death, encodes a protein that activates apoptosis and interacts selectively with survival-promoting proteins Bcl-2 and Bcl-X(L), EMBO J. 16 (1997) (1686-1694).